STRUCTURAL GEOLOGY OF BLACK BUTTE AREA, NORTHWEST EAGLE MOUNTAINS, HUDSPETH COUNTY, TEXAS

by

Donald Dean Edds

B. S., Fort Hays State University, 1984

A MASTER'S THESIS

submitted in partial fulfillment of the

requirements for the degree

MASTER OF SCIENCE

Department of Geology

Kansas State University
Manhattan, Kansas

1987

Approved by:

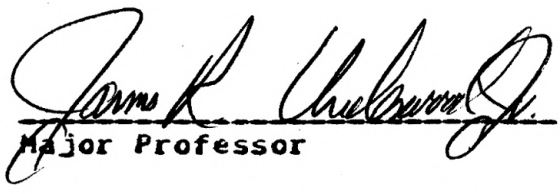

Major Professor

Frontispiece. Southeastward view of Black Butte showing dark-colored Trachyte Porphyry overlying light-colored Lower Rhyolite; syncline in Espy Limestone lies beneath Lower Rhyolite and plunges southeast. Black Butte rises approximately 400 m above alluvium and terrace gravels in the foreground (photograph by J. R. Underwood, Jr.).

CONTENTS

Page

Introduction 1
Purpose of Investigation 1
Location of Study Area 1
Accessibility. 3
Previous Work. 5
Field Procedure. 6
Cartography. 7
Acknowledgments. 7

Physiography 8

Regional Setting 9

Stratigraphy 12
Cretaceous Rocks 12
Tertiary Rocks 16
Quaternary Sediments 17

Competency of Rock Units 18

Folds. 20
Fold Shape 22
Fold Mechanics 24
Deformational Environment of Folding 25

Faults 26
Thrust Faults. 27
Devil Ridge Thrust Fault 27
Minor Thrust Faults. 30
Thrust-Fault Geometry. 33
Strike-slip Faults 34
Normal Faults. 36

Joints 42

Regional Structural History. 43
Pre-Laramide Episodes of Deformation 44
Laramide Deformation 48
Post-Laramide Deformation and Magmatism. 50
Mid-Tertiary Magmatism 50
Basin-and-Range Faulting 51

Structural History of Black Butte Area 52
Laramide Deformation 52
Post-Laramide Deformation and Magmatism. 61
Mid-Tertiary Magmatism 61

Page

Basin-and-Range Faulting 62
Principal-Stess Orientations 65

Comparison of Structural Style with Cieneguilla Area . . 68

Summary. 72

References 74

Appendices 80
Appendix 1. Detailed description of folds in the Black Butte area. 81

ILLUSTRATIONS

Frontispiece. Photograph of Black Butte. i

Figure 1. Location of study area. 2

2. Physiographic features, western Trans-Pecos Texas and adjacent Chihuahua, Mexico. 10

3. Photograph of a fold in the Bluff Formation approximately 1800 m west of Horse Canyon . . 21

4. Photograph showing east-southeastward view of the study area from the southeastern end of Love Hogback 28

5. Classification of thrust systems. 35

6. Late Paleozoic and Mesozoic tectonic features, Trans-Pecos Texas and northeastern Mexico . . 46

7. Diagrams to illustrate migration of arc magmatism and changing tectonic regimes within overriding plate in response to changing dip of subducted slab 49

8. Diagram to illustrate concept of mantle upwelling through slab window to cause uplift and extension of overriding plate 53

9. Photograph of a small fold in the Chispa Summit Formation approximately 1600 m northeast of Pagoda Hill. 56

10. Rose diagrams showing orientations of fold axial traces and thrust-fault traces. 66

TABLES

Table 1. Stratigraphy of Black Butte area. 13

Table 2. Summary of fold data for the Black Butte area . 23

PLATES

Plate 1. Geologic map of Black Butte area, northwest Eagle Mountains, Hudspeth County, Texas. . . . . in pocket

2. Geologic cross sections in Black Butte area, northwest Eagle Mountains, Hudspeth County, Texas. . . . . in pocket

3. Rose diagrams of joint strikes in Black Butte area, northwest Eagle Mountains, Hudspeth County, Texas . . . . in pocket

INTRODUCTION

Purpose of Investigation

This report describes the structural geology of Black Butte area based on a detailed geologic map and cross sections (scale 1:24,000), provides an interpretation of the deformational history based on fold, fault, and fracture relations, and assesses the style of deformation compared with that of the well-studied Cieneguilla area to the south.

The Black Butte region of the Eagle Mountains represents an area where Cretaceous sedimentary rocks have been subjected to at least two different stress regimes: a compressional regime during the Late Cretaceous and early Tertiary, and an extensional regime during the mid-Tertiary.

Location of Study Area

The study area is located in southeastern Hudspeth County, Texas, approximately 25 km southeast of Sierra Blanca and 30 km west-southwest of Van Horn (Fig. 1). The study area is included in the northwest part of the Marfa quadrangle (Barnes, 1979), the northeast corner of the Eagle Mountains Northwest 7.5-minute quadrangle, and the southeast corner of the Grayton Lake 7.5-minute quadrangle. The 50-square-kilometer study area is bounded by latitude 31°00' 29" on the north, an approximate east-west line 1.9 km south of Black Butte on the south, a north-south line through

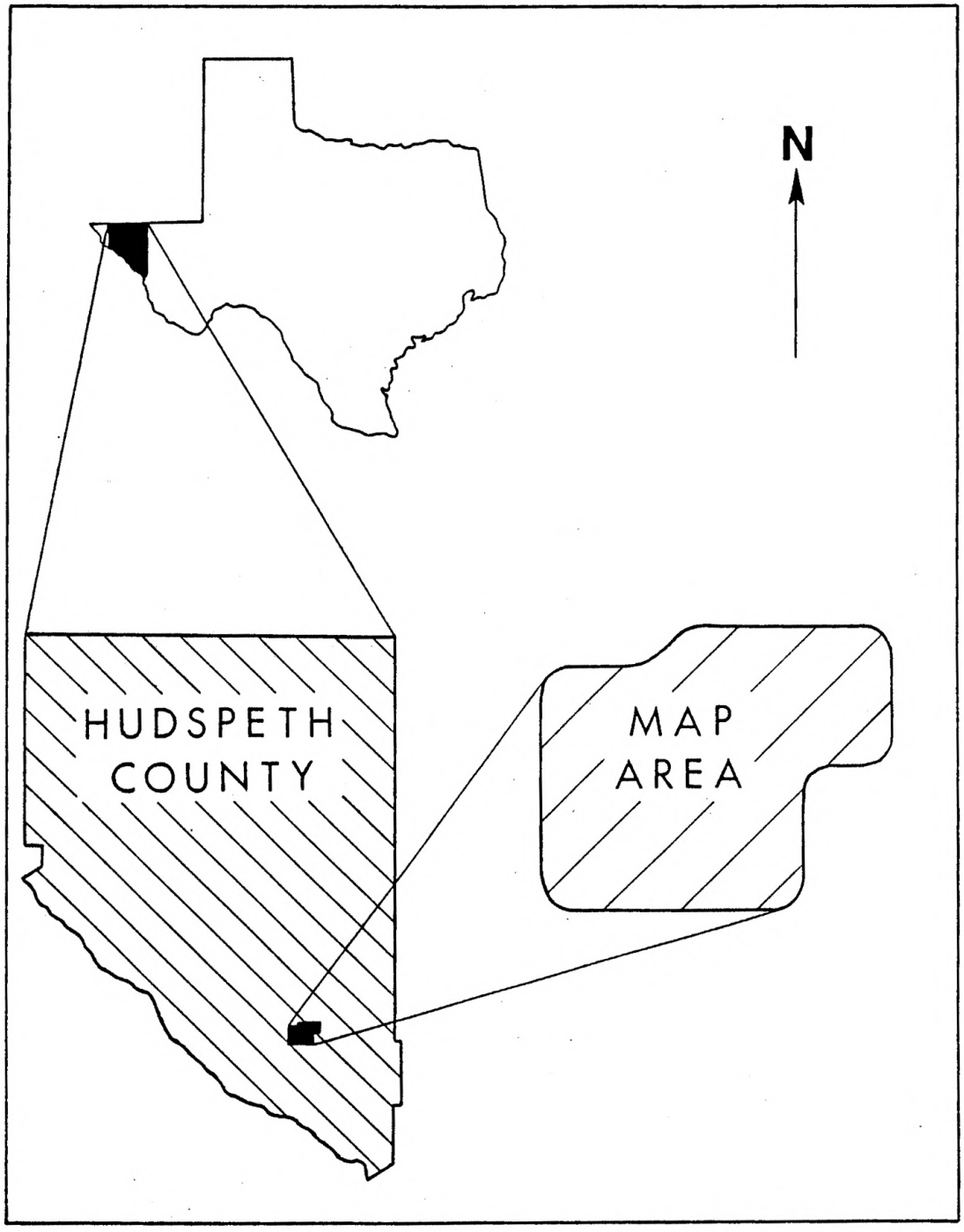

Figure 1. Location of study area.

Horse Canyon on the east, and a north-south line approximately 5.5 km due west of Black Butte on the west.

Black Butte, in the south-central part of the study area, is a relatively small but prominent feature formed from a more resistant Tertiary volcanic sequence overlying a less resistant Cretaceous sequence (Frontispiece). Other prominent features include Speck Ridge to the west and northwest of Black Butte, Red Hills to the northwest of the study area, Red Light windmills to the west of the study area, Love Hogback to the north of the study area, and Pagoda Hill in the north-central part of the study area.

A grid system, shown surrounding the margin of Plate 1, is used to locate features in the map area more accurately. Features are located by a letter-number pair corresponding to the grid square in which the feature is located, .e.g. (F-11). Features that occupy more than one grid square are located by several letters or numbers, .e.g. (F,G-11,12).

Accessibility

Four main routes provide access to the Black Butte area and all require four-wheel-drive vehicles. Access to the northern part of the area is by an unpaved road leaving U.S. Interstate 10 approximately 15.5 km east-southeast of Sierra Blanca, crossing the Southern Pacific railroad tracks 2.4 km south of the interstate and continuing south-southeast through the western part of the Espy Ranch to the Stone

Ranch, and reaching the Stone ranch house at the southeast end of Love Hogback.

The easternmost part of the study area may be reached by an unimproved road that leaves the Stone Ranch road about 5.2 km south of U.S. Interstate 10, continues southeast past the old Jolly place (Underwood, 1962), turns south and extends about 5.6 km to the mouth of Horse Canyon.

Access to the western and southern parts of the area is by an unimproved road leaving the Stone ranch house and continuing west across Goat Arroyo. Just past the southwestern end of Love Hogback the road turns south and continues southeast towards Speck Ridge. At a point 0.5 km northwest of Speck Ridge, the road forks. The right fork leads west-southwest to the western boundary of the study area and the left fork leads southeast along the southwestern flank of Speck Ridge and continues to the southern boundary of the study area.

The southern part of the study area also can be reached by driving south from Sierra Blanca on Ranch Road 1111 to 5-Mile Point where the road forks. The left fork leads southeast and roughly parallels Red Light Draw, the main drainage between the Eagle Mountains and Quitman Mountains. The McMillan Ranch road leads east from Red Light Draw Road about 25 kilometers southeast of 5-Mile Point and continues east approximately 12 km to the McMillan Ranch house, located at the mouth of Frenchman Canyon. An unimproved

road leaves the McMillan Ranch road about 0.5 km west of the McMillan Ranch house and continues northwest to the southern end of Speck Ridge.

Previous Work

Some of the earliest work in and near the Black Butte area was done by Baker (1927). He completed a regional stratigraphic and structural study that covered a large part of southwestern Trans-Pecos Texas, including the Quitman Mountains, the Eagle Mountains region, the Van Horn Mountains, the Wiley Mountains, and Sierra Vieja.

Smith (1940) conducted a stratigraphic and structural study of the Devil Ridge area that included Red Hills and Love Hogback just to the northwest of the map area.

Huffington (1943) studied the geology of the northern Quitman Mountains.

Gillerman (1953), in a report on the fluorspar deposits of the Eagle Mountains, described the structure of the central Eagle Mountains south and east of the study area.

Flawn (King and Flawn, 1953) examined the Precambrian rocks of the Van Horn area, which included those of the Eagle Mountains.

Twiss (1959a and 1959b) reported on the geology of the Van Horn Mountains, the mountain block immediately east of the Eagle Mountains complex.

A Ph.D. dissertation by Underwood (1962) involved a

regional study of the Eagle Mountains, Devil Ridge area, and Indio Mountains and included the Black Butte area. Most of this work was later published (Underwood, 1963).

Albritton and Smith (1965) reported on the geology of the Sierra Blanca area to the northwest of the study area.

King (1965) conducted a geological investigation in the Sierra Diablo region, also north of the study area.

Jones (1968) and Jones and Reaser (1970) studied the geology of the southern Quitman Mountains and vicinity located to the west and southwest of the study area.

A Ph.D. dissertation by Reaser (1974) described the geology of the Cieneguilla area of Chihuahua and Texas. This region also is southwest of the study area.

Field Procedure

A field investigation in the Black Butte area was conducted during the summer of 1985. This began with an examination of all stratigraphic units exposed in the research area at outcrops in and around the area. Fold, fault, joint, and bedding attitudes were determined with a Brunton compass and plotted on 43 x 43-cm aerial photographs, at a scale of 1:24,000. Stereoscopic examination of the aerial photographs aided geologic interpretation. Additional geologic information was obtained from two U.S. Geological Survey 7.5-minute topographic quadrangles: Grayton Lake and Eagle Mountains

Northwest.

Cartography

Geologic information plotted on the aerial photographs was transferred to a larger base map composed of two 96.5 x 96.5-cm aerial photographs at a scale of 1:10,685. Because of the radial distortion of the photographs, the data were transferred to the topographic maps enlarged to a scale of 1:12,000. The final map was prepared by reducing the topographic maps to their original scale of 1:24,000. This produced a map at the desired scale and with enhanced detail but without topographic contours. They became fainter with each recopying until, eventually, they disappeared.

Acknowledgments

I would like to express my appreciation for the assistance provided me by my major professor, Dr. James R. Underwood, Jr., who introduced me to the geology of Trans-Pecos Texas, suggested and guided me in this project, and took time to visit the study area on two separate occasions to familiarize me with the stratigraphy and regional geologic structure of the Eagle Mountains and vicinity. I also wish to thank Messrs. James Stone and Buddy McMillan, Ms. R. H. Espy, and Ms. Lou Selman for allowing access to their land, and the people of the town of Sierra Blanca, Texas for their hospitality. Thanks are extended to Mr. R.

G. McKinney, Gila Exploration, Sante Fe, New Mexico, for providing valuable information on the subsurface stratigraphy and structure in areas near the study area. I owe a special thanks to my parents, Donald and Coleen Edds, for their love, encouragement, and financial support. Graduate study at Kansas State University was supported partly by a graduate teaching assistantship.

The following persons served on the thesis committee and contributed their time and effort in reviewing and editing the manuscript: Dr. James R. Underwood, Jr., Dr. Page C. Twiss, and Professor Emeritus Charles P. Walters, Department of Geology, and Dr. H. L. Seyler, Department of Geography, Kansas State University.

PHYSIOGRAPHY

Topographic relief within the Black Butte area is approximately 610 m. Minimum elevations (1220 m) occur in the extreme southwestern part of the area (M,N-1,2) where Quaternary terrace gravels slope southwestward toward Red Light Draw. Maximum elevations (1830 m) are found in the eastern part of the area (H-13,14) where the Finlay Limestone and Cox Sandstone are in contact with the overlying Lower Rhyolite.

The western part of the study area is covered largely by Quaternary terrace gravels, but several low, north-to-northwest-trending ridges of Bluff and Finlay limestone are

exposed. The central and south-central parts of the area are dominated by Speck Ridge, a prominent northwest-trending ridge of Cox Sandstone and Finlay Limestone, and Black Butte (K-11), a prominent feature capped by a resistant volcanic sequence. Beds of Espy Limestone form low, northwest-trending ridges north of Black Butte.

The part of the study area north of the Devil Ridge thrust fault consists of low, northwest-trending ridges of Espy Limestone, Eagle Mountains Sandstone, and Buda Limestone. The northern and eastern parts of the area that are south of the Devil Ridge thrust fault consist of highly faulted and folded beds of the Yucca Formation, Bluff Formation, Cox Sandstone, and Finlay Limestone and are characterized by high relief. Pagoda Hill (E-9), composed of beds of the Yucca Formation, forms the prominent peak southeast of the Stone ranch house; a series of northwest-to-northeast-trending ridges of Bluff limestone extends from south of Pagoda Hill east to Horse Canyon. Two prominent northwest-trending ridges of Finlay Limestone occur near the northwest edge of the Lower Rhyolite escarpment.

REGIONAL SETTING

The Eagle Mountains region in Hudspeth County, Texas, is part of a mountain range that extends from La Mula, Chihuahua 240 km north-northwestward into Trans-Pecos Texas (Fig. 2). This range is one of a series of subparallel,

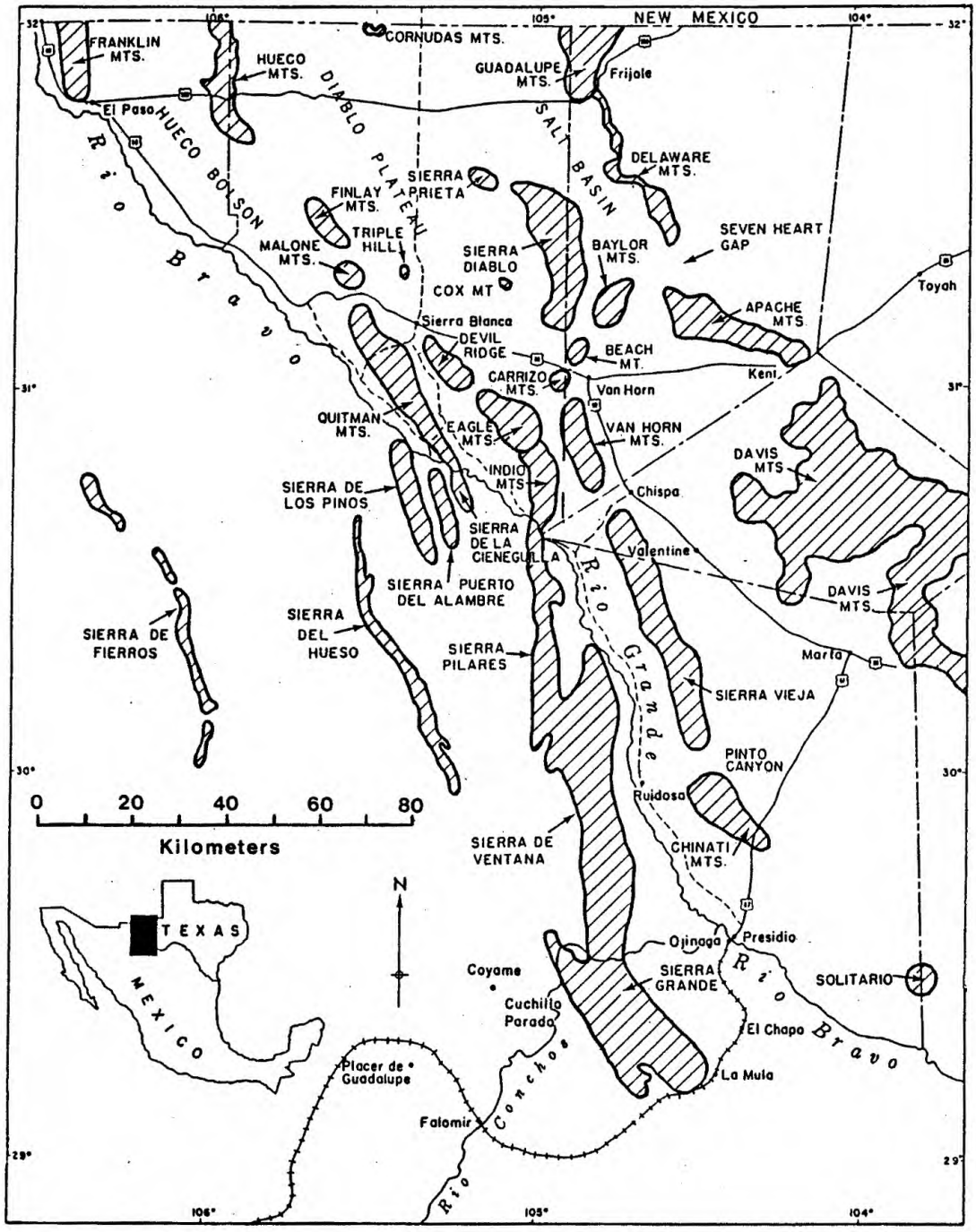

Figure 2. Physiographic features, western Trans-Pecos Texas and adjacent Chihuahua, Mexico (modified after Underwood, 1962).

northwest-trending ranges that are horsts. The intervening basins, some of which are closed basins or bolsons, are grabens (Underwood, 1962). In the Eagle Mountains region, this horst-and-graben structure, produced during Tertiary block-faulting, is superimposed on folds and faults produced earlier during the Laramide Orogeny.

The Eagle Mountains region includes three physiographically distinct, but stratigraphically and structurally related subdivisions (Underwood, 1963): from northwest to south-southwest, Devil Ridge, Eagle Mountains, and Indio Mountains. The Eagle Mountains form the topographically high central portion of the region and are dominantly a Tertiary-age volcanic terrane offset from place to place by normal, thrust, and strike-slip faults. Precambrian metasedimentary rocks and Permian and Cretaceous sedimentary rocks are exposed on the flanks of the mountains. The Devil Ridge area, a northwestward extension, is dominated by a series of hogback ridges where older Cretaceous strata have been thrust onto younger Cretaceous rocks along northwest-trending faults. Small Tertiary intrusive bodies also crop out in the area.

The Indio Mountains are a southeastward extension composed largely of Cretaceous sedimentary rocks, with Tertiary volcanic rocks covering a large area in the southern part of the mountains. Small bodies of Tertiary intrusive rocks occur from place to place in the northern

Indios. The structure in the Indios consists mainly of north-northwest-trending Tertiary normal faults superimposed on a complex of Laramide thrust faults.

STRATIGRAPHY

The stratigraphic sequence in the Black Butte area consists both of Lower and Upper Cretaceous sedimentary rocks, Tertiary volcanic and plutonic igneous rocks, and Quaternary alluvium and terrace gravels (Underwood, 1962). Descriptions of these units are given in Table 1. Precambrian- and Permian-age rocks are exposed in other areas of the Eagle Mountains and vicinity (Underwood, 1962), but do not crop out in the Black Butte area.

Cretaceous Rocks

The oldest rocks exposed in the study area are marine Cretaceous rocks, approximately 2,500 m thick, that range in age from Late Aptian to Late Turonian. The Cretaceous section is characterized by alternating sequences of siliciclastic and calciclastic rocks that were deposited along the eastern margin of the Chihuahua trough (Underwood, 1962). Each formation represents a separate siliclastic or calciclastic unit.

The Yucca Formation, the oldest unit exposed in the map area, is a thick, dominantly siliclastic unit that has a distinctive red-brown color. It consists of a lower unit

SYSTEM	MAP SYMBOL	FORMATION	DESCRIPTION	THICKNESS (METERS)
QUATERNARY	Qal	ALLUVIUM	Silt- to boulder-size sediment of present-day floodplains and stream channels.	——
	Qg (Qg_3, Qg_2, Qg_1)	TERRACE GRAVEL	Qg3, lowest and youngest terrace gravel; Qg1, highest and oldest terrace gravel; Qg, undifferentiated terrace gravel.	——
	QTb	BOLSON FILL	Widespread, older sediment of silt-to-boulder size	——
TERTIARY	Tr	RHYOLITE DIKES AND SILLS	Pale-orange (10 YR 7/2) rhyolite with light-brown (5 YR 5/6) concentrations of iron oxide (<0.1 mm).	——
	Tt	TRACHYTE PORPHYRY	Dark, grayish red (5 R 3/2) trachyte porphyry with white (N9) phenocrysts of alkalic feldspar.	125
	Tlr	LOWER RHYOLITE	Light-gray (N7) rhyolite with medium-gray (N5) microphenocrysts of quartz.	245
CRETACEOUS	Kcs	CHISPA SUMMIT FORMATION	Medium-gray (N5) to black (N1), gypsiferous shale and flaggy limestone grading upward to yellowish gray (5 Y 8/1) mudstone, sandstone, and sandy mudstone.	488
	Kbu	BUDA LIMESTONE	Brownish gray (5 YR 5/1), very finely crystalline, thin-bedded limestone.	73
	Kem	EAGLE MOUNTAINS SANDSTONE	Yellowish brown (10 YR 5/3), very thin-bedded quartz sandstone with limestone and mudstone interbeds. Sandstone is laminated and cross-laminated.	40
	Ke	ESPY LIMESTONE	Brownish gray (5 YR 5/1), very finely crystalline, thin-bedded limestone with mudstone and limestone interbeds.	549
	Kb	BENEVIDES FORMATION	Medium-gray (N5) mudstone overlain by pinkish gray (5 YR 8/1) quartz sandstone. Not exposed in the map area but assumed to be present in the subsurface.	30
	Kf	FINLAY LIMESTONE	Medium-gray (N5), very finely crystalline, thin- to thick-bedded limestone with thin mudstone, siltstone, and quartz-sandstone interbeds. Dictyoconus walnutensis (Carsey) is abundant.	168
	Kcx	COX SANDSTONE	Light-brown (5 YR 6/4) to pale-orange (10 YR 7/2) quartz sandstone with limestone and mudstone interbeds. Sandstone contains intergranular, reddish orange (10 R 6/6) iron oxide (2 mm).	518
	Kbl	BLUFF FORMATION	Medium-gray (N5), very finely crystalline, thin- to thick-bedded limestone with quartz sandstone, mudstone, and oolitic limestone interbeds. Orbitolina sp. is abundant.	365
	Ky	YUCCA FORMATION	Quartz sandstone, conglomeratic sandstone, and conglomerate grading upward to sandstone, siltstone, mudstone, and limestone. Distinctive reddish brown (10 R 4/4) color. Base covered.	305+

Table 1. Stratigraphy of Black Butte area.

composed of quartz sandstone, conglomeratic sandstone, and conglomerate, and an upper unit composed of sandstone, siltstone, mudstone, and limestone. At no place in the Eagle Mountains and vicinity is a complete section of Yucca present. Underwood (1962) estimated an unfaulted thickness of 305 m for the Yucca exposed above the Devil Ridge fault plane in the Devil Ridge area. Because of the reasonably close proximity of the two areas, the same thickness is assumed for the Black Butte area.

The overlying Bluff Formation is a gray, very finely crystalline limestone with interbeds of quartz sandstone, mudstone, and oolitic limestone. A diagnostic characteristic of this unit is the presence, in abundance, of the large foraminifer, Orbitolina sp. A thickness of 365 m was estimated for the Bluff Formation in the area (Underwood, 1962).

The Bluff is overlain by the Cox Sandstone, a quartz sandstone with interbeds of limestone and mudstone. Abundant brown specks, representing intergranular iron oxide, helps distinguish this unit from others in the study area. The thickness was estimated to be about 518 m for the area (Underwood, 1962).

The Finlay Limestone is a gray, very finely crystalline limestone, with thin interbeds of mudstone, siltstone, and quartz sandstone, that is most easily distinguished from other limestone units by the presence in places of the

foraminifer, Dictyoconus walnutensis (Carsey). A thickness of 168 m was estimated for the area (Underwood, 1962).

The Benevides Formation, which is present in other parts of the Eagle Mountains and vicinity, is not exposed in the Black Butte area, although it almost certainly is present. A thickness of 30 m (Underwood, 1962) is assumed to be present in the area.

Overlying the Benevides is the Espy Limestone, a brownish-gray, very finely crystalline limestone with mudstone and limestone interbeds. It is most readily distinguished from other limestone units in the study area by its stratigraphic position and fossil content. Underwood (1962) measured 549 m of Espy in the Devil Ridge area and this is the thickness assumed for the Black Butte area.

The Eagle Mountains Sandstone overlies the Espy and is a yellowish-brown quartz sandstone with interbeds of limestone and mudstone. It is characteristically very thin-bedded as well as laminated and cross laminated. Diagnostic fossils of this unit include Haplostiche texana and Exogyra cartledgi. A thickness of 40 m was determined for the Eagle Mountains Sandstone in the study area.

The Buda Limestone is a brownish-gray, very finely crystalline limestone distinguished from other limestone units in the area by its stratigraphic position and fossil content. A thickness of 73 m was determined for the Buda Limestone in the study area.

The youngest Cretaceous unit exposed in the Black Butte area is the Chispa Summit Formation. It consists of a gray and black, gypsiferous, fissile shale and flaggy limestone at the base that grades upward to mudstone, sandstone, and sandy mudstone. This thick, dark, gypsiferous shale and the presence of Inoceramus sp. help distinguish this unit from others in the study area. Nowhere in the Eagle Mountains and vicinity is a complete section of Chispa Summit present. Underwood (1962) estimated a thickness of 488 m for this unit exposed above the Devil Ridge fault in the Devil Ridge area and this thickness is assumed for the Black Butte area.

Tertiary Rocks

Tertiary volcanic and plutonic igneous rocks also are exposed in the Black Butte area. These include, from oldest to youngest: Lower Rhyolite, Trachyte Porphyry, and numerous rhyolite dikes and sills. The volcanic rocks were extruded during the Oligocene (Jones and Reaser, 1970); the location of their vents remains uncertain.

The Lower Rhyolite is a light-gray unit that forms the lowermost unit of the volcanic sequence exposed in the escarpment along the southeastern margin of the study area, including exposures at Black Butte. Underwood (1962) estimated a thickness of 245 m for the Lower Rhyolite in this area.

The Trachyte Porphyry is a dark, grayish-red unit that

overlies the Lower Rhyolite and forms the cap rock at Black Butte and the smaller peak just to the east. Underwood (1962) measured 226 m of Trachyte Porphyry immediately to the southwest of the study area, west of Indian Springs, but a much thinner exposure, approximately 125 m, exists at Black Butte.

Numerous pale-orange to light-brown rhyolite dikes and sills have intruded the Yucca, Espy, Eagle Mountains, Buda, and Chispa Summit formations southeast and east of the Stone ranch house. These intrusions, no wider than 90 m and averaging 25 m in thickness, parallel fault traces in many localities, suggesting that the magma intruded along fractures.

Quaternary Sediments

The Quaternary alluvium and terrace gravels are scattered throughout the Black Butte area, but they are most widespread in the western half of the area. The alluvium represents younger sediments that lie in the stream beds and on floodplains of the larger tributary streams and drainages.

The terrace gravels represent older sediments that were eroded from adjacent highlands created by late-Tertiary normal faulting. The compositions of these gravels are dependent of the type of rock available in the adjacent mountains.

Following the classification of Underwood (1962), these gravels were mapped from highest and oldest to lowest and youngest as Qg1, Qg2, and Qg3 on Plate 1 and represent succesively lower base levels of the Rio Grande drainage system. They were not identified by lithology but by relative position above the present drainage system (Underwood, 1962).

COMPETENCY OF ROCK UNITS

In the evaluation of the structural deformation in the Black Butte area, an important factor is the competency of the rock units. Competency is a relative property dependent on ductility, thickness, and the tendency of fractures in rock units to heal (Billings, 1972). If two rock units of similar lithology are present in the same stratigraphic section, the thicker unit will be the most competent during deformation (Billings, 1972). In the study area, the stratigraphic section is composed mostly of limestone and quartz sandstone with lesser amounts of siltstone, mudstone, and shale. Experimental deformation of sedimentary rocks under confining pressure (Handin and others, 1976) showed that limestone was significantly more ductile than quartz sandstone because quartz sandstone deforms by microfracturing and macrofracturing, whereas limestone deforms primarily by twin gliding. In addition, Robertson (1960) found that limestone is able to retain its competency

after initial fracturing because of the relative ease by which fractures heal in limestone as compared to quartz sandstone. These data suggest that quartz sandstone, which is more brittle during deformation, would behave more incompetently than limestone in beds of equal thickness. Shales and mudstones are easily deformed and form incompetent rock units when present with less ductile rock units.

The most accurate measure of rock competency in the Black Butte area is relative joint density. In beds of similar thickness, joint density is, on the average, three times greater for quartz sandstone than for limestone. In both lithologies, joint density increases as bedding thickness decreases. Joint planes could not be identified accurately in siltstone, mudstone, and shale; however, fractures are extensive in these units.

Based on these observations, the relative competencies of the rock units in the study area could be estimated. The most competent units are the thick limestone formations: Buda Limestone, Espy Limestone, and Finlay Limestone. These rock units are almost entirely limestone with only the Espy and Finlay containing thin, siliciclastic interbeds. The Bluff Formation is dominantly a calciclastic unit, but would be slightly less competent because of the presence of interbedded quartz sandstone. The Cox Sandstone ranks next in competency because it is dominantly a siliciclastic unit

with interbedded limestone. The Eagle Mountains Sandstone and Benevides Formation are the two thinnest units in the study area and both are dominantly siliciclastic. The fact that they are relatively thin, siliciclastic units makes them more incompetent than the Cox Sandstone. The Yucca Formation is a thick, mostly siliclastic unit like the Cox Sandstone, but would behave less competently because of the presence of more ductile mudstone and siltstone interbedded with the quartz sandstone. The most incompetent rock unit in the study area is the Chispa Summit Formation because of the presence of thick, very ductile shale beds that constitute most of the unit.

FOLDS

Folding in the Black Butte area is characterized by northwest-trending parallel folds, most of which are asymmetric, but some of which are overturned either to the northeast or southwest. Figure 3 shows an anticline in the Bluff Formation that illustrates the open folding typical of folds in the study area.

Overturned folds are present in the extreme western part of the study area, where beds of the Yucca and Bluff formations are involved, and in the Speck Ridge area, where beds of the Cox Sandstone and Finlay Limestone are nearly vertical. Overturned beds were identified by crossbeds and by stratigraphic position.

Figure 3. Northwestward view of an anticline in the Bluff Formation plunging southeast and located approximately 1800 m west of Horse Canyon (F-12). Anticline shows open folding typical of folds in the Black Butte area; thick limestone beds on opposite limbs of the anticline are approximately 20 m apart at the bottom of the photograph.

Asymmetrical folds are distributed throughout the study area with axial traces extending over distances ranging from a few meters to almost 1300 m. Folds within the Chispa Summit Formation northeast of Pagoda Hill have axial traces less than 50 m long and are not shown on Plate 1. Fold data for the Black Butte area are summarized in Table 2; appendix 1 provides additional details of the folds in the study area.

Fold Shape

Major folds of the Black Butte area are open and concentric folds, most of which are asymmetrical and only a few of which are overturned. Underwood (1962) found that open and symmetrical folds typified folds of the Eagle Mountains and vicinity. Most of these folds have broad, rounded hinge areas; dips decrease gradually toward the fold axis. A few of the folds, however, have sharp reversals in dip at the fold axis, ehibiting V-shaped hinge areas. The most notable of these is the syncline of Espy limestone that plunges beneath Black Butte (Frontispiece). Other examples are found in the northwestern fold area where the V-shaped form of two anticlines can be delineated from their outcrop pattern (Plate 1).

Experimental folding of interlayered limestone and quartz sandstone (Handin and others, 1976) showed that in folds where quartz sandstone was the lowermost layer, the

Asymmetrical folds are distributed throughout the study area with axial traces extending over distances ranging from a few meters to almost 1300 m. Folds within the Chispa Summit Formation northeast of Pagoda Hill have axial traces less than 50 m long and are not shown on Plate 1. Fold data for the Black Butte area are summarized in Table 2; appendix 1 provides additional details of the folds in the study area.

Fold Shape

Major folds of the Black Butte area are open and concentric folds, most of which are asymmetrical and only a few of which are overturned. Underwood (1962) found that open and symmetrical folds typified folds of the Eagle Mountains and vicinity. Most of these folds have broad, rounded hinge areas; dips decrease gradually toward the fold axis. A few of the folds, however, have sharp reversals in dip at the fold axis, ehibiting V-shaped hinge areas. The most notable of these is the syncline of Espy limestone that plunges beneath Black Butte (Frontispiece). Other examples are found in the northwestern fold area where the V-shaped form of two anticlines can be delineated from their outcrop pattern (Plate 1).

Experimental folding of interlayered limestone and quartz sandstone (Handin and others, 1976) showed that in folds where quartz sandstone was the lowermost layer, the

Fold Area	Fold Type	Location	Trend	Plunge
Speck Ridge	Syncline	H-10,I-11	N. 40° W.	12° SE.
	Anticline	H-8,I-9	N. 35° W.	22° SE.
	Syncline	H-8,I-9	N. 35° W.	9° SE.
	Syncline	J-10,K-12	N. 45° W.	13° SE.
Northwestern	Anticline	I-2	N.20-55° W.	5° SE.
	Syncline	H,I-2	N.20-55° W.	
	Syncline	H-5	N.10-25° W.	15° SE.
	Syncline	F,G-2	N.15-30° W.	4° SE.
	Anticline	F,G-2	N. 15° W.	7° SE.
	Syncline	F-2	N. 25° W.	15° SE.
	Syncline	E,F-2,3	N. 40° W.	6° SE.
	Anticline	G-3	N. 10° W.	8° SE.
	Anticline	E-3	N. 32° W.	17° SE.
	Anticline	E-4,5	N-N. 30° W.	22° S.
	Syncline	E-5,6	N. 28° W.	5° SE.
Pagoda Hill	Anticline	E-9	N. 43° W.	3° NW.
	Anticline	E-8,9	N. 63° W.	10° NW.
	Syncline	E-8,9	N. 55° W.	8° NW.
	Anticline	F,G-8	N. 13° W.	5° SE.
	Syncline	F,G-8	N. 13° W.	5° SE.
	Anticline	G-9	N. 40° W.	5° SE.
	Syncline	G-9	N. 40° W.	20° SE.
	Syncline	F-10	N. 18° W.	24° SE.
Horse Canyon	Anticline	G-11	N.35-58° W.	3° SE.
	Syncline	G-11	N. 55° W.	17° SE.
	Anticline	F,G-12,13	N. 42° W.	21° SE.
	Syncline	F-12,13	N. 50° W.	7° SE.
	Anticline	F,G-14	N. 22° W.	5° SE.
	Syncline	F,G-14,15	N. 8-33° W.	9° SE.
	Anticline	F-15	N. 35° W.	11° SE.
	Syncline	F-15	N. 60° W.	9° SE.

Table 2. Summary of fold data for the Black Butte area.

fold shape was chevron. In folds where limestone was the lowermost layer, the fold shape was sinusoidal. Therefore, V-shaped (chevron-like) folds in the Black Butte area may have a thick, basal siliciclastic unit that controlled their shape. The rounded (sinusoidal) folds may have a thick, basal calciclastic unit that controlled their shape during deformation.

Small-scale folds in the shale and limestone of the Chispa Summit Formation northeast of Pagoda Hill represent tight folding, probably transitional between concentric and disharmonic (similar) folding. However, true geometric form was difficult to establish in these folds because of intense small-scale faulting that has disrupted the folds.

Fold Mechanics

Folding of most of the Cretaceous units in the Black Butte area was by flexural slip (Donath and Parker, 1964), characterized by slippage of relatively competent beds along bedding planes with no significant change in bed thickness. The competent beds of limestone and quartz sandstone retained their cohesion sufficiently to allow for slip to occur between the layers rather than within the layers.

Minor folds, involving shale and interbedded limestone of the Chispa Summit Formation, show evidence of flexural flow (Donath and Parker, 1964) inasmuch as the shale layers are considerably thicker in the hinge areas than in the

limbs. In this area, cohesion within the layers of shale was less than the adhesion between the layers. Folds that resulted from flexural flow were observed only within beds of the Chispa Summit Formation.

Fold asymmetry in the study area may be related to differences in the amount of bedding-plane slip between the limbs of the fold. Handin and others (1976) experimentally tested multilayered sequences of limestone and quartz sandstone and found that folds were asymmetrical when bedding-plane slip of one of the limbs was restricted by the insertion of tape; the taped limb was shorter and steeper than the untaped limb. In the study area, restriction of bedding-plane slip may have been the result of lateral decreases in bed thickness, faults normal to bedding, or lateral facies changes.

Deformational Environment of Folding

The mechanism of folding that operates in an area is directly related to the deformational environment. Flexural slip was the dominant mechanism of folding in the study area with flexural flow occurring only to a minor degree. According to Donath and Parker (1964), flexural mechanisms are indicative of deformational environments characterized by low-to-moderate pressure and low temperature.

According to Reaser (1982), temperature and pressure during folding in the Cieneguilla-Quitman area, 20 km to the

such as slickensides, cross-cutting relations, attitude of adjacent bedding, and orientations of adjacent folds provided important information on the type of faulting.

Thrust Faults

The majority of northwest-trending faults in the study area are thrust faults. These faults trend parallel or subparallel to adjacent folds in most places and undoubtedly are contemporaneous features. Many of these faults trend parallel to the strike of adjacent beds and although fault plane dips were not determinable in outcrop, many were assumed to be comparable to that of adjacent bedding. Thrust faults were identified by one or more of the following: repetition or omission of strata, reversal of stratigraphic succession without overturning of beds, cross-cutting relations, or abrupt, significant changes in bedding attitude not directly related to folding.

Devil Ridge Thrust Fault.--Evidence for major thrust movement occurs along the Devil Ridge fault in the northern part of the study area where beds of the Yucca Formation, the oldest Cretaceous unit exposed, overlie beds of the Chispa Summit Formation, the youngest Cretaceous unit in the study area (Fig. 4). The fault is exposed at several places in the study area, northwest and east of Pagoda Hill. The attitude of the fault plane could not be determined at any

Figure 4. East-southeastward view from the southeastern end of Love Hogback just to the northwest of the study area; Pagoda Hill, composed of thrust-faulted beds of the Yucca Formation, center; northeastward movement along the Devil Ridge thrust fault at the base of Pagoda Hill brought Yucca into contact with Chispa Summit Formation, largely covered by alluvium and terrace gravels, left foreground and left center; Tertiary volcanic rocks of the Eagle Mountains on the skyline.

of these exposures. Northwest of the study area, just east of Love Hogback and northwest of the Stone ranch house, the fault plane is exposed in a number of places and strikes N. 40° W. and dips an average of 48° southwest.

Northeast-southwest-oriented seismic profiles of areas northwest and southwest of the study area revealed that thrust faults flatten with depth (McKinney, 1986, personal communication) and presumably join a major thrust, or detachment surface, located within the ductile, Permo-Jurassic(?) evaporites. Therefore, an average dip of 25° for the fault plane in the study area is used in calculating displacement along the fault.

Using estimated thicknesses for the Cretaceous units in the area just east of Love Hogback and the presence of about 305 m of Yucca above the fault plane, Underwood (1962) determined the stratigraphic separation to be approximately 2450 m. Therefore, assuming an average dip of 25° and a stratigraphic separation of 2450 m, total displacement along the Devil Ridge fault is about 5800 m.

The east-west trend of the Devil Ridge fault through the Black Butte area is in marked contrast to its overall northwest-southeast orientation throughout other areas of the Eagle Mountains and vicinity. At most exposures of the fault, beds on both sides of the fault dip to the southwest. However, at several localities northwest and east of Pagoda Hill, beds of Chispa Summit and Yucca strike N. 80°-90° E.

and dip to the south and southeast. Most notable of these are the beds within a small klippen of Yucca northwest of Pagoda Hill (D-7,8). The fault plane at this locality presumably dips to the southeast.

Minor Thrust Faults.--Thrust faults in other regions of the Black Butte area are almost entirely restricted to the Cretaceous rocks south and southwest of the Devil Ridge fault and are most extensive within beds of the Yucca Formation. Displacements along these faults range from a few tens to a few hundred meters compared to the estimated nearly 6 km of movement along the Devil Ridge fault.

The Yucca Formation crops out immediately southwest of the Devil Ridge fault in a broad east-west-trending belt that extends from Horse Canyon to the west more than six km. Beds within this outcrop have been cut by a series of dominantly northwest-trending thrust faults. These faults have displacements ranging from several tens to several hundred meters, and were sufficient to thicken the unit considerably.

Based on an estimated, unfaulted thickness of 305 m and an average dip of 20° SW. for the thrust fault planes within the Yucca, maximum total displacement along the fault plane to achieve the fault-thickened section was approximately 800 m. Estimates of this kind apply only to those sections where folding or normal faulting did not significantly

affect the thickness of the section. In areas where beds of Yucca have been repeated, total displacement is distributed among several faults.

A thrust fault northeast of the summit of Pagoda Hill extends southeast from the Devil Ridge fault (D-8), as a diverging splay (Boyer and Elliot, 1982), and intersects a northeast-trending normal fault southeast of Pagoda Hill (E-9). The thrust fault extending southeast from this normal fault, from a point northeast of the intersection, may be an extension of the splay.

A second thrust fault near the base of Pagoda Hill on the northeast slope, also extends southeast, as a splay, from the Devil Ridge fault (D-9), and rejoins the fault to the southeast (E-10). According to Boyer and Elliot (1982), this fault would be classified as a rejoining splay.

The Yucca just west of Horse Canyon is dissected by a series of west-northwest-to-northwest-trending thrust faults. The northernmost of these thrusts are inferred to merge with the Devil Ridge fault as splays to the northwest. The southernmost of these faults terminate to the northwest and southeast against northeast-trending normal faults and cannot be traced beyong them.

A thrust fault, splaying from the Devil Ridge fault approximately 600 m east of Pagoda Hill (E-10), extends south and east beneath a northwest-trending ridge capped by Bluff limestone. The fault parallels the Yucca-Bluff

contact along the ridge. Yucca has been thrust over Bluff along the southeast end of the fault (F-12) and displacement there is approximately 500 m. A small splay branches off this fault near its southeast end, extends east-northeast approximately 400 m and merges into the thrust fault to the northeast (F-12). This splay serves as a connective splay (Boyer and Elliot, 1982) by joining the two thrust faults.

Approximately 2 km due west of Pagoda Hill, beds of the Bluff Formation dipping 50°-56° SW. overlie beds of Cox Sandstone dipping 25°-30° SW. along a northwest-trending thrust fault (E-5,6). Near the southeast end of the fault, older beds of Bluff overlie younger beds of Bluff. The trace of this fault is believed to extend southeast beneath the Quaternary sediments and splay into a pair of northeast-trending thrust faults exposed north of Speck Ridge along which limestone of the Bluff Formation has been thrust.

Immediately west of Horse Canyon, the Bluff Formation and Cox Sandstone are exposed in a narrow east-west-trending ridge bounded on the north and south by normal faults. Beds of Bluff, exposed at the east end of the ridge, have been repeated by a pair of closely-spaced, northwest-trending thrust faults (F,G-15). West of these faults, along a third northwest-trending thrust fault (F,G-14) beds of the Bluff Formation have been thrust over beds of the Cox Sandstone.

The large exposure of Cox Sandstone west of Horse Canyon and north of the Lower Rhyolite escarpment

(G,H-13,14,15) has been faulted by several northwest-trending thrust faults. Along the northwesternmost of these faults, Cox Sandstone, dipping steeply to the northeast, has been thrust over younger beds of Cox Sandstone, dipping gently to the southwest.

A thrust fault located north of the Devil Ridge thrust fault is exposed within beds of the Espy Formation near the northeast corner of the study area (C-14). This fault is inferred to extend southeast, beneath the Quaternary sediments, and to become truncated by the Devil Ridge thrust fault. This is the only thrust fault known north of the Devil Ridge fault within the study area.

Thrust-Fault Geometry.--Movement along the Devil Ridge thrust fault represents the greatest fault displacement within the Black Butte area. Thrusting in other areas of the Black Butte region was minor compared to thrusting along the Devil Ridge fault.

In a regional context, most of the study area is part of a large thrust sheet that has been transported nearly six km to the northeast along the Devil Ridge fault. The arrangement of the minor thrust faults within the thrust sheet is typical of an imbricate thrust system. The Devil Ridge fault represents a sole thrust, the lower common thrust in an imbricate system (Dennis, 1967), and the minor thrust faults constitute the imbricate fan.

According to Boyer and Elliot (1982), the Devil Ridge thrust system would be classified as a leading imbricate fan (Fig. 5) as the thrust with maximum slip is at the leading edge. The Red Hills thrust fault, exposed in the Devil Ridge area, parallels and lies to the southwest of the Devil Ridge fault and shows displacement nearly equal to that of the Devil Ridge fault (Underwood, 1962). The Red Hills fault can be traced southeast to the Red Hills, just northwest of the study area, but its extent to the southeast is unknown.

According to the thrust-front classification of Morley (1986), the Devil Ridge thrust system is a strongly emergent thrust front. In this type of thrust front, the sole thrust ramps to the surface, and the thrust sheet displays development of internal deformation followed by overthrusting of the entire deformed sheet several kilometers.

Strike-Slip Faults

Evidence for strike-slip movement in the Black Butte area is present in three separate areas where adjacent beds, dipping in opposite directions as a result of folding or faulting, are offset in the same direction. These faults trend N. 35°-90° E. and have displacements ranging from 35 m to 130 m.

A right-lateral strike-slip fault, trending

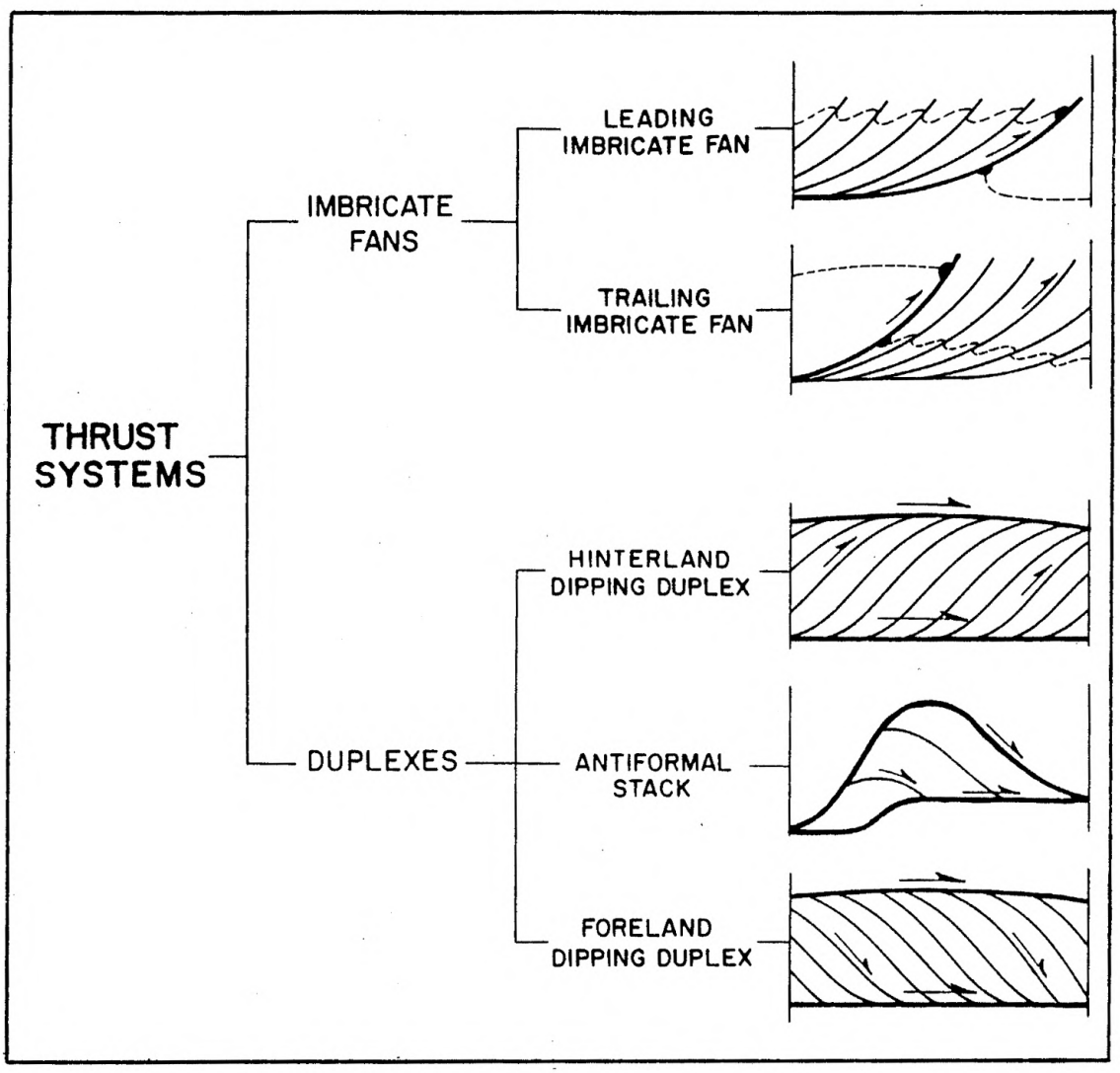

Figure 5. Classification of thrust systems (after Boyer and Elliot, 1982).

N. 35°-90° E., offsets folds in the northwestern fold area (F-2,3). Beds of the Yucca and Bluff formations are offset approximately 35 m along the fault.

The near-vertical beds of Finlay Limestone, Cox Sandstone, and Bluff Formation that extend northwest from beneath the cover of volcanic rock in the eastern part of the study area (H-13) are offset by a left-lateral strike-slip fault, trending N. 25°-80° E. Displacement along this fault is about 130 m.

Steeply-dipping beds of Finlay Limestone and Cox Sandstone in the southern part of Speck Ridge (K-10) are offset by a left-lateral strike-slip fault, trending N. 70°-90° E. Displacement along this fault is approximately 80 m.

Normal Faults

The dominant trend of normal faults in the study area is northeast; the secondary trend is northwest. These faults are vertical or near-vertical with displacements ranging from a few meters to a few hundred meters. Normal faults with displacements of 10 m or less are not discussed.

A normal fault trending N. 75° E. offsets the northwest-trending beds of the foreland area of the Devil Ridge thrust fault (C-11,12). The southeast block has gone down relative to the northwest block. Beds adjacent to the fault dip, on the average, 25° SW., and lateral offset of

the beds is approximately 175 m. Therefore, normal displacement is approximately 80 m.

Southeast of this fault and southeast of the rhyolite sill separating the Buda Limestone and Eagle Mountains Sandstone (C-13,14) a normal fault, trending N. 65° E. shows a lateral offset of 50 m. As beds in the area of the fault dip 23° SW., vertical displacement is about 20 m; the northwest block has moved down relative to the southeast block.

A normal fault, northwest block down, trending N. 50° E., offsets beds of the Chispa Summit Formation, Buda Limestone, and Eagle Mountains Sandstone in the extreme northern part of the study area (C-10,11) and extends north of the map area. Lateral offset along this fault is 70 m and beds adjacent to the fault dip 25° SW. Therefore, vertical displacement is approximately 33 m.

In the area south of the Devil Ridge fault, west of Pagoda Hill (E-7), a normal fault trending N. 45°-55° E. offsets beds of the Yucca Formation. The fault trace parallels, and is adjacent to, a narrow rhyolite dike. Horizontal separation of the thrust fault offset by the normal fault is 100 m, and the dip of adjacent bedding is 40° SW. Therefore, displacement along the fault is about 85 m.

West of this fault, near the northern boundary of the map area (D-5,6), beds of Cox Sandstone dipping about 45° SW

are in contact with beds of the Yucca Formation having similar dips along a fault trending northeast at its western end and northwest at its eastern end. Normal displacement must have been at least 365 m, south block down, along most of the length of the fault to account for the missing Bluff.

Southeast of Pagoda Hill, a normal fault trending approximately N. 55° E. offsets beds of the Yucca Formation and extends from the Yucca-Bluff fault contact (F-8) northeast to the Yucca-Chispa Summit fault contact (E-10). Displacement along this fault could not be accurately determined because of the lack of stratigraphic correlation of units on both sides of the fault. A thrust fault extending southeast from this normal fault may be an extension of the thrust fault to the northwest. If this is so, normal displacement is about 90 m, southeast block down.

A third normal fault with significant displacement located within the Yucca Formation extends from the Yucca-Bluff contact, southeast of Pagoda Hill (F-10), N. 67° E. to the Devil Ridge fault (E-12). Displacement along this fault was found to be about 15 m, southeast block down.

Southeast of the southwest end of this fault, a northwest-trending ridge consisting of beds of the Bluff Formation is offset by a pair of closely-spaced normal faults trending northeast (F-11). Along the northwesternmost of these faults, the northwest block has moved down approximately 10 m, relative to the southeast

block. Along the southeasternmost fault, the southeast block has moved down approximately 25 m, relative to the northwest block.

East of this pair of faults is a second pair of normal faults trending north to northwest. The northwest fault extends from the Bluff-Finlay fault contact on the southwest (F-12) to the northern edge of the Yucca outcrop (E-13) and shows a displacement of about 10 m. The southeast fault extends from the Bluff-Yucca thrust-fault contact on the southwest (F-13) to approximately the same location as the northwest fault at the northern edge of the Yucca outcrop (E-13). Displacement along this fault is about 20 m, southeast block down.

A nearly east-west-oriented ridge of beds of the Bluff Formation and Cox Sandstone extends westward from Horse Canyon and is bounded on the north and south by normal faults (F,G-14,15). Along the northern fault, beds of the Yucca Formation are in contact with beds of Cox Sandstone. The southern block must have moved down at least 365 m relative to the northern block to account for the missing Bluff Formation. This fault turns and extends southwest to the Bluff-Cox contact (G-13) where displacement is about 50 m. Along the normal fault south of the ridge, Cox Sandstone of the southern block is in contact with beds of the Bluff Formation and Cox Sandstone of the northern block. Displacement along this fault is about 50 m.

This fault extends west to a normal fault trending N. 45°-90° E. (G-13; F-14). This northeast-trending fault has offset the Cox-Bluff contact nearly 75 m. Inasmuch as beds near the fault on its northeast end dip, on average, 45° SW., displacement is approximately 75 m. Near the western end of the fault, Cox Sandstone dipping steeply northeast is in contact with beds of the Bluff Formation dipping to the northeast. Beds on the south side of the fault have moved down about 365 m.

A normal fault trending N. 45° W. and dipping 75° SW. transects the ridge (F-15) and is truncated on both ends by east-west-trending normal faults. Cox Sandstone dipping 35°-50° SW. on the southwest block is in contact with beds of the Bluff Formation dipping approximately 70° NE. Displacement is estimated to be about 335 m, southwest block down.

A northwest-trending ridge of Finlay Limestone extends northwest from beneath the volcanic cover, approximately 1250 m west of Horse Canyon (G-13). Beds of Finlay Limestone form the southwest part of the ridge, strike N. 45° W., and dip steeply to the southwest. Limestone of the Bluff Formation forms the northeast part of the ridge, strikes N. 45° W., and dips steeply to the northeast or is vertical. The units are in contact along a normal fault along which the southwest block has moved down at least 518 m to account for the missing Cox.

Extending west-southwest from the northwest end of this fault (G-10,11,12) is a normal fault along which beds of the Bluff Formation are in contact with the Finlay Limestone. The minimum displacement must be at least equal to the thickness of the missing Cox Sandstone, i.e., approximately 518 m. This fault is believed to extend west-southwest to an east-west-trending fault in an exposure of Cox Sandstone near the north end of Speck Ridge (G-8,9). Overturned beds of Cox Sandstone dipping approximately 85° SW. south of the fault are in contact with beds of Cox Sandstone dipping 40° SW. north of the fault and displacement is approximately 430 m, south block down.

A major northwest-trending normal fault traverses the length of Speck Ridge. Steeply-dipping, overturned beds of Finlay Limestone of the southwest block are in contact with northeast-dipping beds of Finlay Limestone of the northeast block, northwest of the strike-slip fault. Displacement along this part of the fault is about 190 m, southwest block down. Southeast of the strike-slip fault, beds of the southwest block dip gently to the southeast. Displacement along this part of the fault is about 230 m, southwest block down.

The Lower Rhyolite and Trachyte Porphyry in and around Black Butte have been offset by normal movement along a fault which had laterally offset the southern part of Speck Ridge during an earlier period of strike-slip movement.

Normal displacement could not be accurately determined, but an estimate of 10 m is not unreasonable.

Due west of the southern part of Speck Ridge an outcrop of beds of the Bluff and Yucca formations is dissected by several northeast-trending normal faults. The second of these from the northwest end (L-6) shows a lateral offset of 40 m. The dip of beds in this outcrop is 30° NE., so displacement is about 23 m, northwest block down.

JOINTS

Joint data (183 joints) collected in the study area were used to aid in the determination of the orientation of the maximum principal stress during Laramide deformation. Most of the joint attitudes were measured on joints having planar surfaces and belonging to well-developed joint sets. In places where the attitude of the joint surface could not be measured and only the trace of the joint was present, the dip of the joint was assumed to be perpendicular to the bedding plane. It is assumed that most of the joints formed when the beds were horizontal or nearly so and that the two dominant joint directions represent shear-fracture directions oriented 30° on either side of the maximum principal stress (Anderson, 1951). Bedding planes of beds containing the joints were rotated to the horizontal using a stereonet, and the rotated joint strike direction was determined. The strikes of the rotated joints were

determined for six localities in the study area: Pagoda Hill, the northern part of Speck Ridge, the east-west ridge extending west of Horse Canyon, the area southeast of peak 4796 in the northeastern part of the study area, the exposure of Bluff Formation, west of the southern part of Speck Ridge, and the large outcrop of the Bluff and Yucca formations in the northwestern fold area (Plate 1). Each of these localities included joint measurements within a 500 m radius of the selected center points. The data from each locality were grouped into 10-degree intervals and plotted on rose diagrams (Plate 3).

The two dominant joint directions measured for each locality are as follows: Pagoda Hill, N. 15° W. and N. 55° E.; the northern part of Speck Ridge, N. 5° E. and N. 75° E.; the east-west-trending ridge extending west of Horse Canyon, N. 15° E. and N. 70° E.; the area southeast of peak 4796, N. 15° E. and N. 80° E.; the exposure of Bluff Formation, west of the southern part of Speck Ridge, N. 25° E. and N. 75° E.; and the large outcrop of the Bluff and Yucca formations in the northwestern fold area, N. 25° E. and N. 75° E.

REGIONAL STRUCTURAL HISTORY

Workers in the region have identified at least five major tectonic episodes that affected rocks in the Eagle Mountains region. Two of these episodes were pre-Laramide

and thus did not involve rocks exposed in the Black Butte area.

Pre-Laramide Episodes of Deformation

During the late Precambrian, the region was part of a geosyncline, the Van Horn mobile belt, on the Texas craton (Flawn, 1956). In the Eagle Mountains region, sedimentary and igneous rocks of the Carrizo Mountain Group were deformed and metamorphosed within the geosyncline (King and Flawn, 1953) approximately 1220 Ma ago (Reynolds, 1985). Following this event, rocks of the Carrizo Mountain Group were thrust northward over the Precambrian Allamore and Hazel formations along the Streeruwitz fault, severely deforming and metamorphosing the Allamore and Hazel formations (King and Flawn, 1953). Evidence for this deformation is found in Precambrian rocks exposed on the northeast flank of, and in various outcrops north and east of, the Eagle Mountains. Muehlberger and others (1967) suggested that this deformation and metamorphism were related to the Grenville Orogeny involving a continent-to-continent collision. Following this event, in the late Precambrian, the region is interpreted to have been characterized by rifting that extended almost continuously around the North American craton (Stewart, 1976).

Goetz and Dickerson (1985) believed that during the late Precambrian through Paleozoic, the region was part of a

northwest-trending transform zone bounded on the south by the Mohave-Sonora megashear (Silver and Anderson, 1974) and connecting the north-striking western plate edge with the margin of the proto-Atlantic coast. According to Goetz and Dickerson (1985), the Paleozoic depositional basins and uplifts were produced by transpressive and transtensional motion, along faults parallel to the transform margin, to accomodate the oblique application of stress. Transpression is transcurrence combined with compression and transtension is transcurrence combined with extension (Harland, 1971). A proto-Chihuahua trough had developed in the Late Mississippian (Gries, 1980; Goetz and Dickerson, 1985) in approximately the same location as the later Chihuahua trough.

Beginning in the Early Pennsylvanian, thrusting and deformation in the Marathon orogenic belt resulted in a series of uplifts and basins in the foreland area to the north and west (King, 1965). The Eagle Mountains region was located on the northeastern edge of the Chihuahua trough near the southwestern edge of the Diablo platform. According to Haenggi and Gries (1970), "... the major Mesozoic tectonic elements of northeastern Chihuahua and adjacent Trans-Pecos Texas (Diablo, Coahila, and Aldama platforms, and the Chihuahua trough) (Fig. 6) all had their inception during Carboniferous time." Kluth and Coney (1981) have interpreted the Paleozoic uplifts in this region

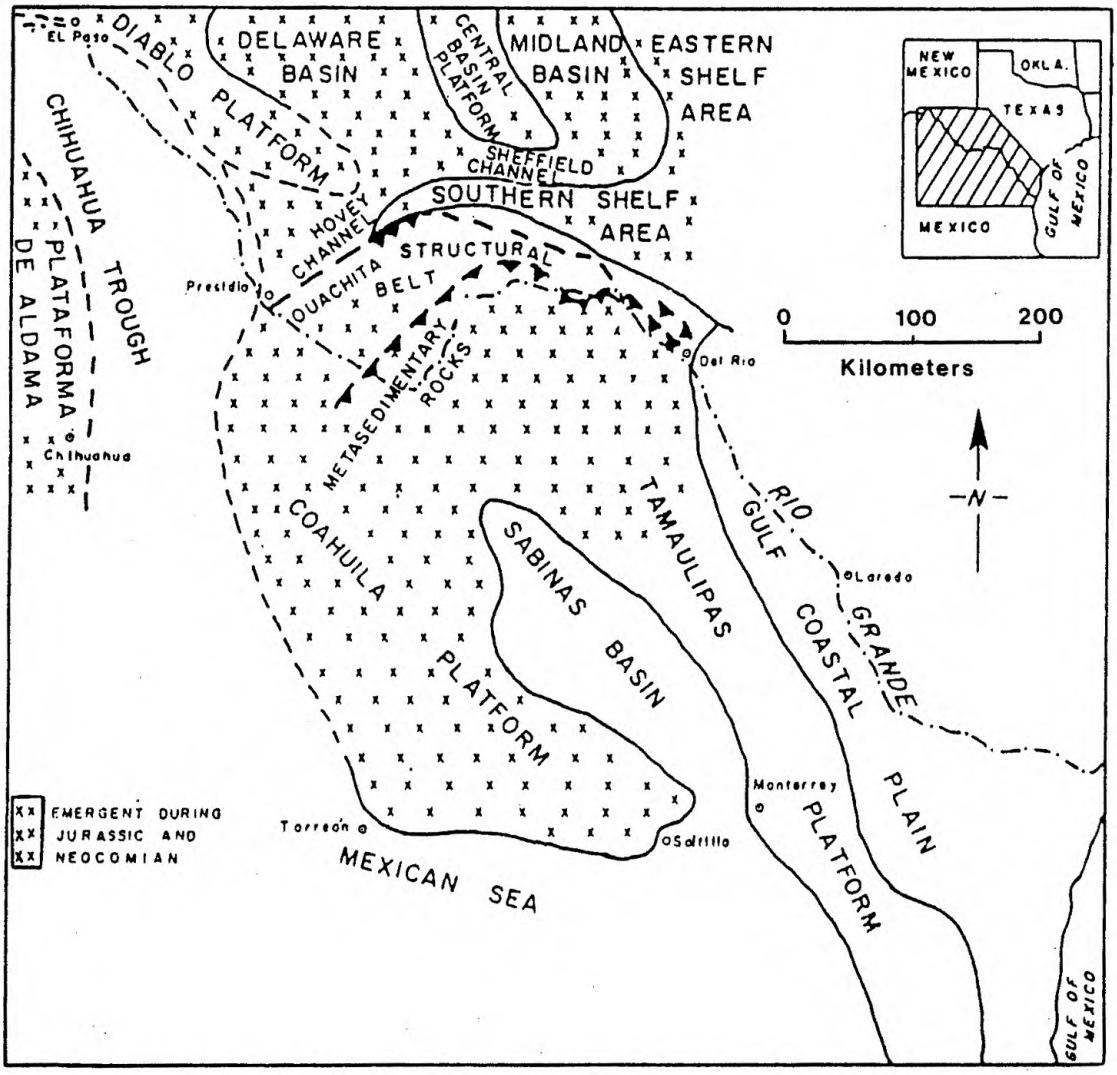

Figure 6. Late Paleozoic and Mesozoic tectonic features, Trans-Pecos Texas and northeastern Mexico (after Haenggi, 1966).

to be the southernmost expressions of the Ancestral Rocky Mountains because of the similar presumed origins for the two areas. Dickinson (1981) proposed that the Chihuahua trough continued to develop by extension and subsidence during the Late Jurassic and Cretaceous in a back-arc area of the Farallon-North American arc system; however, little evidence is available to support this model. Berge (1982) found evidence for a Late Triassic to Early Jurassic normal-faulting event that formed the Chihuahua trough. These normal faults, described in the Malone Mountains approximately 35 km to the northwest of the Black Butte area, cut Permian, but not Jurassic strata (Berge, 1982).

Sedimentation within the Chihuahua trough began in the Late Jurassic (Gries and Haenggi, 1970) with the deposition of an evaporite sequence. This evaporite sequence is known from outcrops and drilled subsurface sections throughout northeast Chihuahua and adjacent Trans-Pecos Texas. Although Underwood (1962) did not find evidence supporting the presence of evaporites in the Eagle Mountains and vicinity, recent exploratory drilling in the area (McKinney, 1986, personal communication) verified their presence in the subsurface a few kilometers northwest of the Black Butte area.

During the Cretaceous, the Chihuahua trough subsided as sediments accumulated from the adjacent Aldama and Diablo platforms. In the Eagle Mountains region, about 2500 m of

Cretaceous rocks were deposited along the eastern margin of the Chihuahua trough (Underwood, 1962). Reaser and Underwood (1975) believed that more than 6100 m of sedimentary rock were deposited in the deepest parts of the trough.

Laramide Deformation

The Laramide Orogeny affected the western part of North America during the Late Cretaceous to late Eocene (Dickinson, 1981) and involved subduction of the Farallon plate beneath the North American plate. Coney (1976) and Dickinson and Snyder (1978) believed that a shallow mode of subduction, as evidenced by the existence of the Paleogene magmatic null in the Cordillera, was directly responsible for the Laramide Orogeny. In addition, a decrease in the angle of subduction for the southern Cordillera during the Laramide is suggested by the eastward migration of arc magmatism and compressional deformation toward the interior of the continent (Fig 7a)(Coney, 1978; Dickinson and Snyder, 1978). Relative motion between the two plates was probably oriented northeast-southwest (Coney, 1976).

This northeast-southwest oriented compression deformed the sediments of the Chihuahua trough forming the Chihuahua tectonic belt (Deford, 1958), dominated by a series of northwest-trending ranges. Overthrusting, overturning, and asymmetry of folds in the eastern part of the Chihuahua

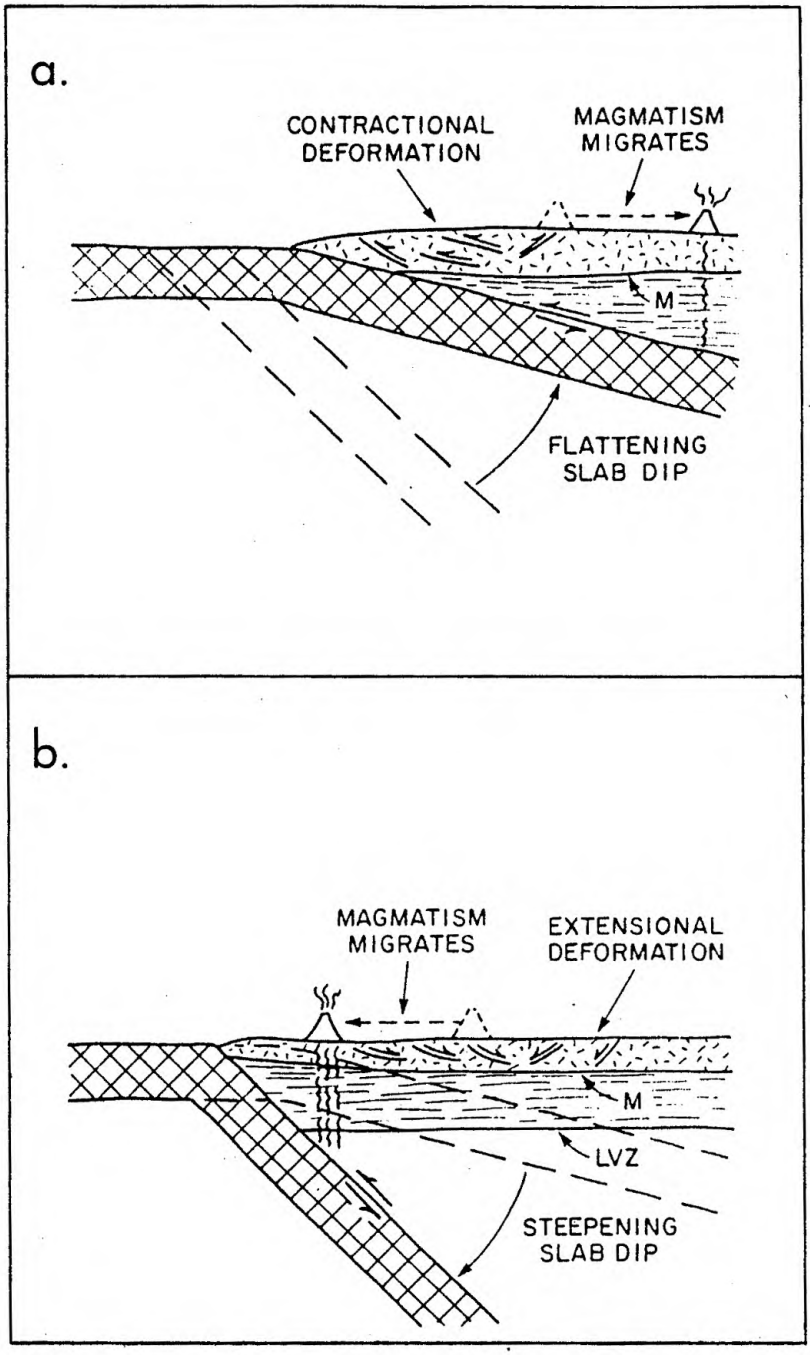

Figure 7. Diagrams to illustrate migration of arc magmatism and changing tectonic regimes within overriding plate in response to changing dip of subducted slab. (a) Arc magmatism and contractional deformation migrate eastward toward the interior of the continent as slab dip decreases. (b) Arc magmatism and extensional deformation migrate westward as slab dip increases. M, Moho; LVZ, low-velocity zone (modified after Dickinson, 1981).

tectonic belt are mostly northeastward toward the Diablo platform suggesting that this platform acted as a buttress during Laramide deformation (Reaser and Underwood, 1975).

Thrusting in the Chihuahua tectonic belt was most likely initiated along a décollement zone. Deford (1964) stated that the complex folding of Cretaceous limestone in the mountains of the Chihuahua tectonic belt suggested the presence of underlying salt or anhydrite. Gries and Haenggi (Haenggi, 1966; Gries and Haenggi, 1969; Gries, 1970; Haenggi and Gries, 1970; Gries and Haenggi, 1970; Gries, 1980) believed that Cretaceous rocks in the Chihuahua trough were intensely deformed along a décollement zone of Jurassic(?) evaporite during the Laramide Orogeny. In addition, the structural style of the Cieneguilla area was believed to be the result of décollement-style tectonics (Reaser, 1974).

Post-Laramide Deformation and Magmatism

Mid-Tertiary Magmatism.--Igneous rocks were intruded and extruded in the Eagle Mountains region from late Eocene to early Oligocene (Jones and Reaser, 1970). Henry and McDowell (1986) found that igneous activity in the Tertiary Trans-Pecos magmatic province was dominated by mafic-to-silicic magmas between 38 and 32 Ma ago. These magmas are the easternmost of an eastward sweep of magmatism that began near the paleotrench, which lay off western Mexico, at least

100 Ma and reached Texas about 40 Ma (Coney and Reynolds, 1977). The tectonic setting of the Trans-Pecos magmatic province has been interpreted as being related to subduction in a continental-arc environment (Lipman and others, 1972) or in a back-arc environment (Barker, 1979). Price and Henry (1984) argued that compression during the period of vulcanism was essentially the same as that during Eocene Laramide deformation and thus supported a continental-arc tectonic setting.

Twiss (1959) and Underwood (1962) found that, in places, Tertiary igneous rocks were tilted or gently warped and attributed this to a late period of compression or subsidence that accompanied the extrusion of igneous rock. Henry and Price (1984) also found evidence for subsidence in the region, and related it to caldera collapse.

Basin-and-Range Faulting.--Beginning in the middle Oligocene the region was uplifted several thousands of meters and block faulted (Deford and Bridges, 1959). Haenggi and Gries (1970) suggested that the interior zone of the Chihuahua tectonic belt was not involved in the block faulting. Only in a 32-km-wide belt extending from El Paso-Juarez to south of Presidio-Ojinaga has block faulting been superimposed on Laramide structural features (Deford and Bridges, 1959).

Zoback and others (1981) believed that the uplift and extension that accompanied block faulting in the southern

Basin-and-Range province was the result of back-arc spreading caused by continued subduction of the Farallon plate at a steep angle (Fig. 7b). Dickinson and Snyder (1979) argued that the absence of a subducted slab and the upwelling of asthenosphere through the slab window may have initiated uplift and extension within the Basin-and-Range province (Fig. 8).

The block faulting produced a series of north- to north-northwest-trending mountain blocks, bounded by large-scale normal faults. Underwood (1962) found evidence of large-scale normal faults separating Cretaceous rock from bolson sediment in the Eagle Mountains and vicinity. Additional evidence of large-scale normal faults bounding and cutting mountain blocks exists in other areas of the region.

STRUCTURAL HISTORY OF BLACK BUTTE AREA

Laramide Deformation

Northeast-southwest-oriented compression during the Laramide Orogeny resulted in northwest-trending folds and thrust faults and northeast-trending strike-slip faults. Evidence from one locality in the Black Butte area suggests that folding preceeded thrust faulting. The anticline and syncline located within limestone beds of the Bluff Formation, approximately 1200 m southwest of the summit of

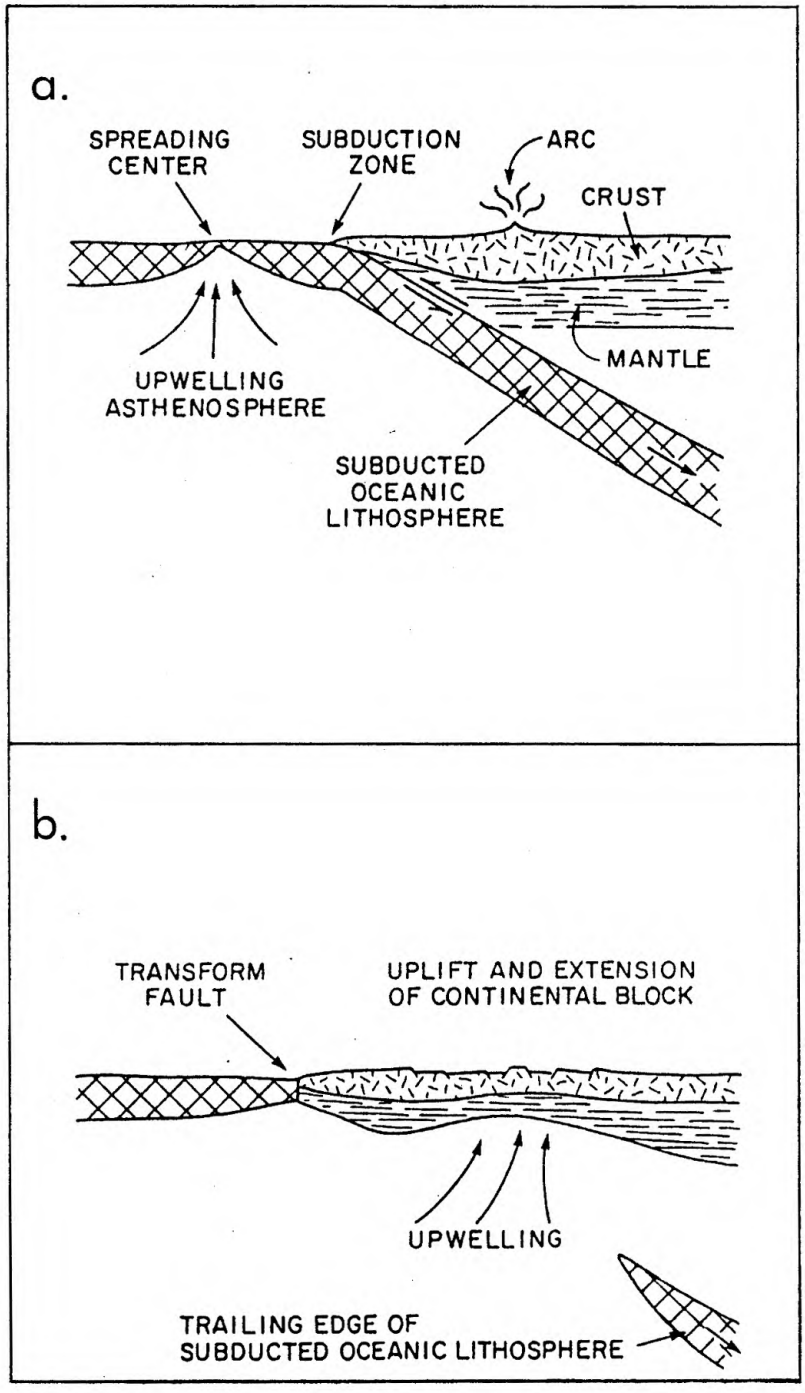

Figure 8. Diagram to illustrate concept of mantle upwelling through slab window to cause uplift and extension of overriding plate. (a) Oceanic spreading rise approaches subduction zone. (b) Encounter of rise and trench has produced transform fault as trailing edge of subducted slab continues to descend, thus producing slab window through which asthenosphere then rises (after Dickinson, 1981).

Pagoda Hill (F,G-8), are truncated on their northwest ends by a northeast-trending thrust fault; the fold axes cannot be traced into the overridden block. Therefore, folding in this area must have occurred prior to the latest movement along the fault.

In other localities within the study area fold and fault relations seem to suggest that folding and thrust faulting occurred at approximately the same time. In general, for these areas, fold axes are parallel or subparallel to adjacent thrust faults. Many of the smaller folds may have formed in response to drag along the faults during thrusting.

The small anticline within the Yucca Formation immediately east of the summit of Pagoda Hill (E-9) is adjacent to, and on the overthrust block of, the thrust fault to the northeast. The position and alignment of the anticline relative to the fault suggests that the fold may have been produced by drag of the overthrust block against the underthrust block.

The fold pair approximately 1100 m south-southeast of Pagoda Hill (G-9) is located within beds of the Bluff Formation on opposite sides of a thrust fault. The position and close proximity of the folds relative to the fault suggests that they may have formed by drag along the fault. A similar relationship is found near the west end of the ridge extending west of Horse Canyon where the anticline,

southwest of the fault (F,G-14), is in the overthrust block and the syncline, northeast of the fault (F,G-15), is in the overridden block. These folds also may be the result of drag along the fault during thrusting to the northeast. Similarly, the syncline, located approximately 850 m southeast of Pagoda Hill and within beds of the Bluff Formation (F-10), roughly parallels the thrust fault to the southwest and is probably a drag fold.

The minor folds within the Chispa Summit Formation (Fig. 9) northeast of Pagoda Hill (D-11,12) probably are related to movement along the Devil Ridge fault. These folds are more than 450 m north of the fault and could not have been produced by drag along the fault directly. However, the more competent beds of the Chispa Summit Formation must have transmitted shear stresses, produced by movement along the fault, a considerable distance into the foreland area. Although other folds within the Chispa Summit Formation were not found in the study area, they must be present beneath the Quaternary sedimentary cover.

Other folds in the Black Butte area do not show direct evidence of being related to movement along adjacent thrust faults. This conclusion is based on one or more of the following: large fold amplitudes relative to the inferred displacement along the fault; asymmetry to the southwest, opposite to the inferred direction of thrusting; location of the folds at distances greater than a few tens of meters

Figure 9. East-southeastward view of a small fold in the Chispa Summit Formation approximately 1600 m northeast of Pagoda Hill (C-11). This fold is one of a series of small folds in the Chispa Summit Formation formed in response to northeastward movement along the Devil Ridge thrust fault.

from the thrust faults; or folds oriented oppositely to those produced from drag along southwest-dipping thrust faults.

In the Speck Ridge area, thrusting to the northeast along the fault that traverses the length of the ridge probably accompanied folding immediately northeast and southwest of the ridge, inasmuch as fold axes parallel the inferred thrust-fault trace. Drag may account for only a relatively minor amount of the folding in this area.

Evidence for thrust faulting preceeding folding was not found in the study area as folded thrust contacts were not identified. The steep, near-vertical fault planes of the three southwesternmost listric faults (Section C-C'; Plate 2) may be the result of tilting or rotation of the fault planes following thrusting. Boyer and Elliot (1982, p. 1199) stated that thrust faults of imbricate systems "... can meet the ground surface at about 60°." However, it is uncertain whether this value represents an average or a theoretical maximum value based on a homogeneous rock section. If this is a maximum value, then the near-vertical dips of these thrust-fault planes probably are the result of tilting of the fault planes. However, the stratigraphic section in the study area is quite clearly not homogeneous. Therefore, the near-vertical dips may be the original dips and simply represent above-average values.

Dahlstrom (1969) provided an interpretation for thrust

fault-fold relations in imbricate thrust systems. He showed how a thrust fault could lose displacement upsection by transferring its displacement to a progressively-developing fold at its tip; a decrease in fault displacement upsection is balanced by an increase in fold-related shortening. In this interpretation, the anticlines of the Black Butte area would be underlain or traversed along their axes by thrust faults. The fault traversing the northwest-trending ridge west of Horse Canyon may fit this interpretation. In addition, the larger anticlines that are asymmetrical to the northeast may be fault-tip anticlines.

The determination of relative ages of thrusting in the study area is difficult because apparent truncations possibly may represent splays formed contemporaneously with major thrusts. The Devil Ridge fault, which trends approximately east-west across the study area, truncates all but one of the minor thrust faults, and movement along the Devil Ridge fault was greater than that of any other in the area. This suggests that movement along the minor thrusts predated movement of the entire thrust sheet. Morley (1986) found that deformation within thrust sheets prior to movement of the entire thrust sheet was characteristic of strongly emergent thrust fronts.

The northwest trend of fault traces and folds and the northwest strike of beds throughout most of the area suggest that movement of the thrust sheet was northeast. At several

places along the Devil Ridge fault the trace assumes an east-northeast orientation and beds adjacent to the fault stike east-northeast. These areas may represent areas where thrusting was locally northwest, but more simply may reflect the irregular surface onto which the rocks were thrust. It is also possible that older, pre-Laramide zones of weakness were reactivated during northeast-southwest-oriented compression.

The present east-west trace of the Devil Ridge fault through the study area is probably the result of erosion that removed much of the overthrust block in the area north of Pagoda Hill and exposed a large area of Chispa Summit Formation of the underthrust block. This interpretation would require that the fault is an erosion thrust or that the fault cuts upsection and intersects beds stratigraphically higher within the Chispa Summit Formation from east to west across the study area.

Strike-slip faults offset or truncate folds, thrust faults, and high-angle faults along which earlier thrusting is believed to have occurred in the Black Butte area. Apparently, these faults represent the latest deformational event associated with Laramide compression.

Folds in the northeastern fold area are offset by a right-lateral strike-slip fault (F-2,3). Beds of the southwest limb of the southwesternmost syncline show a marked change in strike from about N. 10° W. northwest of

the fault to about N. 15° E. southeast of the fault. This difference may be the result of drag along the fault during lateral movement.

South-southeast of this series of folds, in an exposure of beds of the Bluff Formation (I-2), beds show a change in strike from N. 20° W. to N. 50° W. proceeding southeast through the outcrop. This change in strike may be the result of drag during left-lateral motion on a northeast-trending strike-slip fault located southeast of this outcrop beneath the Quaternary sediments.

The left-lateral strike-slip fault west of Horse Canyon (H-13) offsets beds of Finlay Limestone dipping steeply to the southwest, limestone beds of the Bluff Formation dipping steeply to the northeast, and beds of the Cox Sandstone dipping southwest and northeast. The fault also offsets the high-angle fault that traverses the length of the ridge, along which earlier thrusting is believed to have occurred. The strike-slip fault is believed to extend east-northeast beneath the volcanic cover and laterally offset the syncline within the Espy Limestone.

The strike-slip offsets of the northwest-trending high-angle faults at Speck Ridge and the ridge west of Horse Canyon provide additional evidence for a Laramide origin for the high-angle faults.

Post-Laramide Deformation and Magmatism

Mid-Tertiary Magmatism.--Igneous rocks were intruded and extruded in the Black Butte area concurrent with intrusion and extrusion in other areas of the Eagle Mountains region (Underwood, 1962); this igneous activity began sometime after 38 Ma ago and terminated sometime before 32 Ma ago (Henry and McDowell, 1986). The volcanic rocks in the study area represent the northwesternmost volcanic rocks exposed in the Eagle Mountains and vicinity. Exposures of volcanic rocks are confined to the southeastern part of the study area, but the thickness, approximately 370 m, suggests that much, if not all, of the study area was overlain by volcanic rock.

Dikes and sills of rhyolite parallel normal faults from place to place in the area, suggesting that magma intruded fractures formed during earlier Laramide compression. Inasmuch as many of the dikes and sills are offset by normal faults, the intrusion of rhyolite probably predated the main episode of Basin-and-Range faulting in the area. On the other hand, the unfaulted rhyolite dikes and sills northwest and northeast of Pagoda Hill may have postdated the period of normal faulting. Faulting of the volcanic rocks in and around Black Butte also suggests that the extrusion of igneous rock preceded the main episode of normal faulting.

Basin-and-Range Faulting.--Normal faulting of the area in the mid-Oligocene occurred in response to northeast-southwest-oriented Basin-and-Range extension. Deformation was characterized mostly by movement along northeast-southwest-oriented, high-angle faults, most of which probably formed as shear fractures during Laramide compression, and by movement along reactivated, northwest-trending faults, probably originating as thrust faults during the Laramide Orogeny. In many places, the normal faults offset or truncate thrust faults and strike-slip faults.

In some areas, however, normal faults are apparently truncated by thrust faults. The northwest-trending normal fault west of the summit of Pagoda Hill and paralleling the rhyolite dike within the Yucca Formation offsets a thrust fault to the northeast and is truncated by a thrust fault on its northeast end (D-8). Its termination against the thrust fault represents the limit of normal displacement and signifies that normal movement was restricted to the overthrust block of this fault. This, in turn, is probably a reflection of the extent of the shear fracture produced during Laramide compression.

A similar relationship is found along the normal fault just to the southeast of Pagoda Hill (E-9). This fault truncates and possibly offsets several thrust faults along its trace, but terminates abruptly on both ends, against

thrust faults, one of which is the Devil Ridge fault. These faults mark the limit of normal displacement and, most likely, the limit of earlier shear fracturing. Two of the thrust faults appear to be truncated and have no extension southeast of the normal fault. This may indicate that the normal fault served as a strike-slip boundary for the thrusts during the Laramide Orogeny. It may be that the traces are present southeast of the fault and were just not identified. The fault relationships observed along this fault are found also in other localities in the study area.

The presence of northeast-trending normal faults north of the Devil Ridge fault indicates that high-angle faulting was not restricted to the thrust sheet but affected the foreland area as well. Nowhere in the Black Butte area do normal faults offset the Devil Ridge fault at the surface. This may be because shear fractures planes were restricted to separate fault blocks or because of widespread Quaternary sedimentary rocks concealing possible fault traces in the area near the fault. Offset of the Devil Ridge fault by normal faults is inferred in the subsurface (Section B-B'; Plate 2).

Normal displacement also occurred along northwest-trending high-angle faults in the study area. These faults probably formed in response to northeast-southwest oriented extension along extension fractures and were characterized by relatively short traces and small displacements (Plate 1)

and were inferred to have planar surfaces (Plate 2). Two of the northwest-trending normal faults apparently were reactivated faults along which earlier thrusting occurred.

A high-angle fault traverses the length of the northwest-trending ridge of Finlay Limestone west of Horse Canyon (G-13). Normal movement, southwest block down, placed the Finlay Limestone southwest of the fault against beds of the Bluff Formation northeast of the fault. This fault has a relatively large trace, parallels thrust faults in the area, and is offset by a strike-slip fault near its southeast end, suggesting a Laramide origin for the fault. Thus, it is inferred to flatten with depth (Section C-C'; Plate 2).

The northwest-trending fault traversing the length of Speck Ridge shows evidence for normal movement as southwest-dipping beds of Finlay Limestone southwest of the fault are adjacent to northeast-dipping beds of Finlay Limestone northeast of the fault. The southwest block must have moved down relative to the northeast block, presumably along the same fault plane along which earlier thrusting occurred (Sections B-B', C-C', and D-D'; Plate 2).

Southeast of the strike-slip fault, in the southern part of the ridge and in the vicinity of Judge Triangulation Station, beds of Finaly Limestone and Cox Sandstone are not overturned but dip 25°-40° SE. This abrupt change in attitude across the strike-slip fault is interpreted to be

the result of a greater amount of normal movement along the northwest-trending fault. South of the northeast-trending fault that transects the ridge, beds near the crest of the anticline are in contact with the steeply dipping southwest limb of the syncline (Section E-E'; Plate 2).

Principal-Stress Orientations

Structural trends within the Black Butte area were analyzed to determine the principal-stress orientations. Fold axes and thrust-fault traces, assumed to be oriented perpendicular to the maximum compressive stress orientation, provided the most accurate indicators. As the dips of the fault planes were not known for most of the thrust faults, only 23 faults with fairly straight, horizontal traces were used in the analysis. It was assumed that the trends of these faults more closely approximated strike directions.

The trends of fold axes were determined and plotted in Figure 10a. A dominant trend of N. 35° W. for these structures indicates that the maximum principal compressive stress that produced them was oriented N. 55° E.

Thrust fault trends were determined and plotted in Figure 10b. A dominant trend of N. 40° W. for these structures indicates that the maximum principal compressive stress that produced them was oriented N. 50° E.

Joint data were also used in determining principal compressive stress directions (Plate 3). These data show an

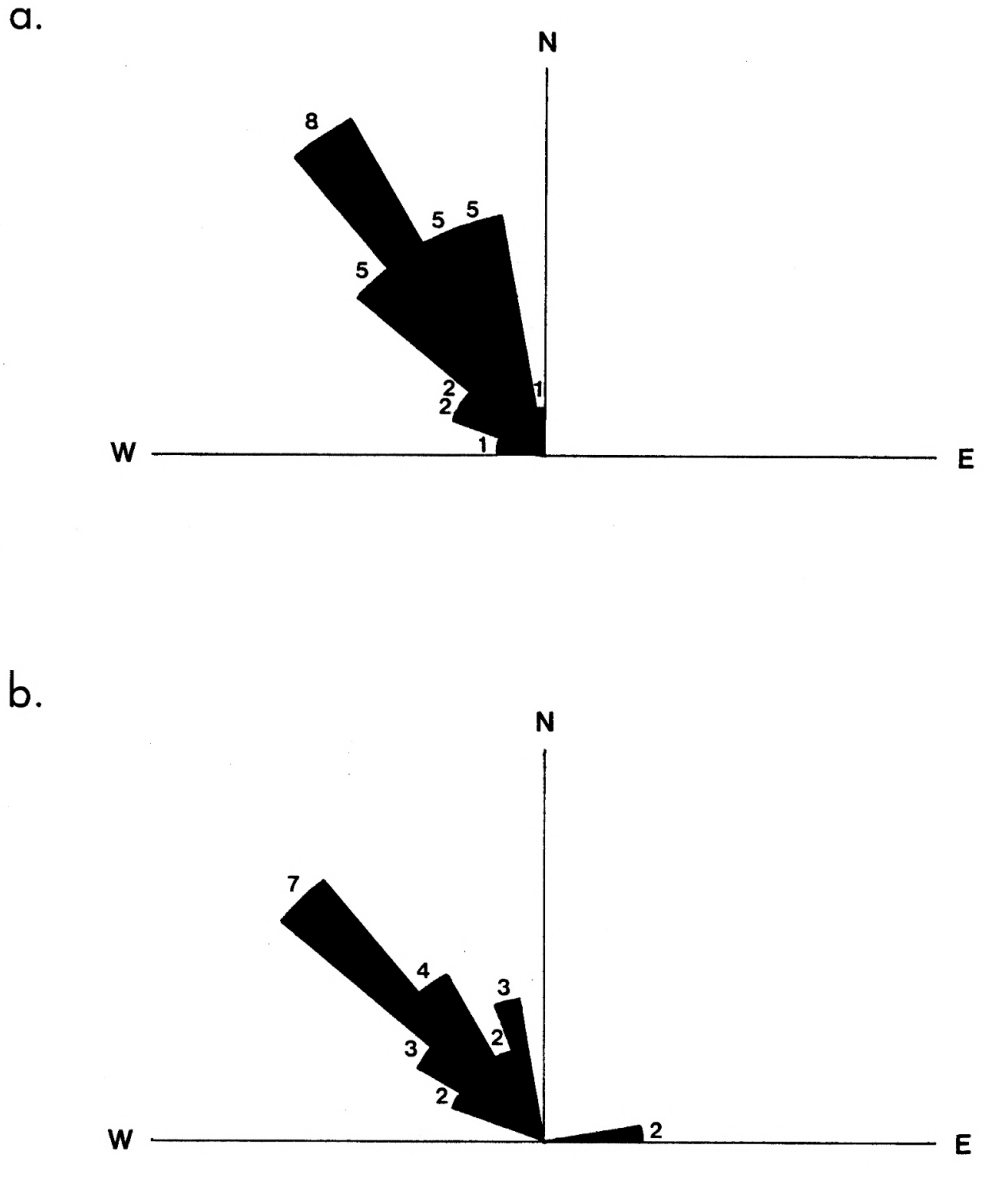

Figure 10. Rose diagrams showing orientations of (a) fold axial traces and (b) thrust fault traces. Numbers represent the actual number of traces measured in a 10-degree interval.

average of about N. 40° E. for the maximum principal compressive stress orientation.

During folding and thrusting, the least principal stress orientation was vertical and the intermediate principal stress orientation was northwest. Locally, during strike-slip faulting the least principal stress was oriented northwest and the intermediate principal stress was oriented vertically.

Price and Henry (1984) argued for two separate periods of Laramide compression in Trans-Pecos Texas: an early compression oriented northeast and a later compression oriented east-northeast. Their argument was partly based on the presence of refolded folds in the Malone Mountains and folded thrust faults in the Indio Mountains. However, the lack of conclusive evidence for two separate compressional events and the fairly narrow range of values of the maximum principal compressive stress determined for the Black Butte area suggests that only a single compressional event operated in the area.

During Basin-and-Range extension, the maximum principal stress was vertical, the least principal stress was oriented northeast-southwest, and the intermediate principal stress was oriented northwest-southeast.

COMPARISON OF STRUCTURAL STYLE WITH CIENEGUILLA AREA

The Cieneguilla area, located approximately 20 km south of the Black Butte area, is part of a structural trend in the Chihuahua tectonic belt that includes the southern end of the southern Quitman Mountains of Texas and Sierra Cieneguilla of Chihuahua, Mexico (Fig. 2). Like the Black Butte area, the Cieneguilla area is characterized by Cretaceous sedimentary rocks of the Chihuahua trough that have been folded and faulted in response to Laramide compression (Reaser, 1974). The two areas can be instructively compared because: (1) rocks of the Cieneguilla area were deposited in the Chihuahua trough farther from the craton than those of the Black Butte area; (2) the environment of deformation (temperature and pressure) in the Cieneguilla area was more intense than that of the Black Butte area; (3) the deformed rocks of the Cieneguilla area are well exposed; and (4) these rocks have been described in detail (Jones and Reaser, 1970; Reaser, 1974; Reaser and Underwood, 1975).

Structurally, the Cieneguilla area is part of a large-scale, northwest-trending overturned (nearly recumbent) anticline, the Cieneguilla-Quitman anticline, upon which numerous small folds have been superimposed (Reaser, 1974). Folding in the area is characterized mostly by tight, overturned-to-recumbent folds, ranging in form from sharp,

cheveron-like Z-shaped folds to rounded, S-shaped and broad "horseshoe" folds, as viewed in cross section (Reaser, 1974). Reaser (1974) also described disharmonic folds within the Finlay Limestone and Espy Limestone.

These folds are in strong contrast to those of the Black Butte area where folds are more widely-spaced and generally open and asymmetrical. Disharmonic folding in the Black Butte area apparently was restricted to the Chispa Summit Formation.

A considerable contrast in the type and intensity of faulting between the two areas also is evident. Reaser (1974) found "no clearly defined, large-scale thrust faults separating strata in the Cieneguilla area," but only "small-scale bedding-surface thrusts mostly confined to the Espy Formation and associated with tight minor folds." Strike-slip movement on several northeast-trending, high-angle faults was the dominant type of displacement associated with Laramide compression in the area (Reaser, 1974). Faulting in the Black Butte area was dominated by imbricate thrust faults present at several stratigraphic levels, but most numerous in the Yucca Formation. Strike-slip faulting occurred only to a minor degree in the area.

Major, northwest-trending normal faults bound the Cieneguilla area (Jones and Reaser, 1970) as they are inferred to do in the Eagle Mountains and vicinity (Underwood, 1962). Numerous, northeast-trending normal

faults occur in the Cieneguilla area as well as in the Black Butte area. Thus, Basin-and-Range extension in the Cieneguilla area was not significantly different from that of the Black Butte area and surrounding Eagle Mountains area.

The differences in Laramide structural styles between the two areas can be attributed to the presence of a much thicker Permo-Jurassic(?) evaporite sequence in the Cieneguilla area. An increase in the thickness of the Cretaceous section from northeast to southwest is well documented for the area (Twiss, 1959; Underwood, 1962; Jones and Reaser, 1970); this increase reflects a progression toward the center of the Chihuahua trough. It follows that accumulation of some of the earliest sediments, Permo-Jurassic(?) evaporites, also attained a maximum thickness in the center of the trough.

The role of the thick evaporite sequence in the Cieneguilla area was apparently two-fold (Reaser, 1974). During Laramide compression, the evaporite sequence served as a zone of dislocation along which décollement-style thrusting occurred. The Cieneguilla-Quitman anticline began developing in response to this compression, and growth of the anticline continued as evaporite flowed from the trough of adjacent synclines to the core of the anticline. Further movement along the décollement zone resulted in the formation of the complex series of folds on the overturned

limb. Thus, the evaporite played a passive role in serving as a décollement zone and an active role in contributing to the growth of the anticline.

The thinner evaporite sequence in the Black Butte area apparently served only as a glide plane along which thrust faults developed. The thinned and possibly absent evaporite sequence in the study area may explain why thrust faults are present in the Black Butte area and not in the Cieneguilla area. In the Cieneguilla area, shortening was accommadated by flowage of the evaporite sequence. In the Black Butte area, with the absence of a décollement to the northeast, displacement was transferred upsection from the evaporites to the Lower Cretaceous section along the Devil Ridge fault and its associated minor faults.

SUMMARY

The structural development of the Black Butte area was controlled mainly by deformational environment, the influence of regional structural features, and lithology. During the late Paleozoic the study area was part of, and on the northeast edge of, the Chihuahua trough, a basin formed as the result of uplift of the Aldama platform to the southwest and the Diablo platform to the northeast. Sedimentation within the trough began with the deposition of a Permo-Jurassic(?) evaporite sequence and was followed by the depostion of more than 2,500 m of Lower and Upper Cretaceous rocks in the study area. Northeast-southwest-oriented compression during the Laramide Orogeny deformed the sediments of the trough resulting in the formation of northwest-trending folds and thrust faults and northeast-trending strike-slip faults in the area. Major thrust movement in the area occurred along the Devil Ridge fault. An estimated 6 km of northeastward movement along this fault placed beds of the Yucca Formation, the oldest Cretaceous unit, against beds of the Chispa Summit Formation, the youngest Cretaceous unit. Minor northwest-trending thrust faults, confined mostly to the Yucca Formation within the Devil Ridge thrust sheet, constitute the imbricate fan. All of the thrust faults are believed to flatten with depth and join a major sole thrust or zone of dislocation within the

ductile Permo-Jurassic(?) evaporites. Folding in the area is characterized by open and rounded concentric folds, most of which are asymmetrical, either to the northeast or southwest, but some of which are overturned. This type of folding suggests that deformation occurred in a near-surface environment, not deeper than 2.5 km. Temperature and pressure during deformation probably ranged from near-surface conditions to 625 bars pressure and 75°C temperature. Following a period of vulcanism in the mid-Tertiary, northeast-southwest-oriented extension produced a series of normal faults, most of which trend northeast, probably originating as shear fractures during Laramide compression. A few of the normal faults trend northwest and are believed to have originated as thrust faults during the Laramide Orogeny.

Thrust faulting dominates the structural style of the Black Butte area, whereas folding has been the dominant mode of deformation in the Cieneguilla area, some 20 km to the south. This difference in structural style can be attributed to the presence of a much thicker Permo-Jurassic(?) evaporite sequence, serving as a zone of dislocation for décollement-style tectonics and as an active element in the development of large-scale, complex folds in the Cieneguilla area.

REFERENCES

Albritton, C.C., Jr., and Smith, J.F., Jr., 1965, Geology of the Sierra Blanca area, Hudspeth County, Texas: U.S. Geological Survey Professional Paper 479, 131 p.

Anderson, E.M., 1951, The dynamics of faulting: Edinburgh, Oliver and Boyd, 206 p.

Baker, C.L., 1927, Exploratory geology of a part of southwestern Trans-Pecos Texas: Texas University Bureau of Economic Geology Bulletin 2745, 70 p.

Barker, D.S., 1979, Cenozoic magmatism in the Trans-Pecos province: Relation to Rio Grande rift, in Riecker, R.E., ed., Rio Grande rift: Tectonics and magmatism: Washington, D.C., American Geophysical Union, p. 382-392.

Barnes, V.W., ed., 1979, Marfa Sheet, Geologic Atlas of Texas: Texas University Bureau of Economic Geology.

Berge, T.B., 1982, Structural evolution of the northeastern Chihuahua tectonic belt, in Powers, R.B., ed., Geologic studies of the Cordilleran thrust belt, v. 1: Rocky Mountain Association of Geologists, Denver, Colorado, p. 451-457.

Billings, M.P., 1972, Structural geology, 3rd ed.: Englewood Cliffs, Prentice-Hall Inc., 606 p.

Boyer, S.E., and Elliot, D., 1982, Thrust systems: American Association of Petroleum Geologists Bulletin, v. 66, no. 9, p. 1196-1230.

Coney, P.J., 1976, Plate tectonics and the Laramide orogeny, in Woodward, L.A., and Northrop, S.A., eds., Tectonics and mineral resources of southwestern North America: New Mexico Geological Society Special Publication 6, p. 5-10.

Coney, P.J., 1978, Mesozoic-Cenozoic Cordilleran plate tectonics, in Smith, R.B. and Eaton, G.P., eds, Cenozoic tectonics and regional geophysics of the western Cordillera: Geological Society of America Memoir 152, p. 33-50.

Coney, P.J., and Reynolds, S.J., 1977, Cordilleran Benioff zones: Nature, v. 270, no. 5636, p. 403-406.

Dahlstrom, D.C.A., 1969, Balanced cross sections: Canadian Journal of Earth Science, v. 6, no. 4, p. 743-757.

Deford, R.K., 1958, Cretaceous platform and geosyncline, Culberson and Hudspeth counties, Trans-Pecos Texas: Society of Economic Paleontologists and Mineralogists, Permian Basin Section, Field Trip Guidebook, 90 p.

Deford, R.K., 1964, History of geologic exploration in Chihuahua: West Texas Geological Society Guidebook, Publication 64-50, p. 116-129.

Deford, R.K., and Bridges, L.W., 1959, Tarantula Gravel, northern Rim Rock Country, Trans-Pecos Texas: Texas Journal of Science, v. 11, no. 3, p. 286-295.

Dennis, J.G., 1967, International tectonic dictionary: American Association of Petroleum Geologists Memoir 7, 196 p.

Dickinson, W.R., 1981, Plate tectonic evolution of the southern Cordillera, in Dickinson, W.R., and Payne, W.D., eds., Relations of tectonics to ore deposits in the Southern Cordillera: Arizona Geological Society Digest, v. 14, p. 113-135.

Dickinson, W.R., and Snyder, W.S., 1978, Plate tectonics of the Laramide orogeny, in Matthews, Vincent, III, ed., Laramide folding associated with basement block faulting in the western United States: Geological Society of America Memoir 151, p. 355-366.

Dickinson, W.R., and Snyder, W.S., 1979, Geometry of subducted slabs related to the San Andreas transform: Journal of Geology, v. 87, no. 6, p. 609-627.

Donath, F.A., and Parker, R.B., 1964, Folds and folding: Geological Society of America Bulletin, v. 75, no. 1, p. 45-62.

Flawn, P.T., 1956, Basement rocks of Texas and southeast New Mexico: Texas University Bureau of Economic Geology Publication 5605, 261 p.

Gillerman, E., 1953, Fluorspar deposits of the Eagle Mountains, Trans-Pecos Texas: U.S. Geological Survey Bulletin 987, 98 p.

Goetz, L.K., and Dickerson, P.W., 1985, A Paleozoic transform margin in Arizona, New Mexico, West Texas, and northern Mexico, in Dickerson, P.W., and Muehlberger, W.R., eds., Structure and tectonics of Trans-Pecos Texas: West Texas Geological Society Publication 85-71, p. 173-184.

Gries, J.C., 1970, Geology of the Sierra de la Parra area, northeast Chihuahua, Mexico: University of Texas, Austin, Ph.D. dissertation, 151 p.

Gries, J.C., 1980, Laramide evaporite tectonics along the Texas-Northern Chihuahua border, in Dickerson, P.W., ed., Trans-Pecos region: New Mexico Geological Society 31st Field Conference Guidebook, p. 93-100.

Gries, J.C., and Haenggi, W.T., 1969, Structural development of the eastern Chihuahua tectonic belt, northeastern Chihuahua, Mexico (abs): Geological Society of America Abstracts for 1969 Annual Meeting, no. 1, p. 83.

Gries, J.C., and Haenggi, W.T., 1970, Structural evolution of the eastern Chihuahua tectonic belt: West Texas Geological Society symposium, p. 119-137.

Haenggi, W.T., 1966, Geology of El Cuervo area, northeastern Chihuahua, Mexico: University of Texas, Austin, Ph.D. dissertation, 403 p.

Haenggi, W.T., and Gries, J.C., 1970, Structural evolution of northeastern Chihuahua tectonic belt: Society of Economic Paleontologists and Mineralogists, Permian Basin Section, Publication 70-12, p. 55-69.

Handin, J., Friedman, M., Min, K.D., and Pattison, L.J., 1976, Experimental folding of rocks under confining pressure: Part II. Buckling of multilayered rock beams: Geological Society of America Bulletin, v. 87, no. 7, p. 1035-1048.

Harland, W.B., 1971, Tectonic transpression in Caledonian Spitzbergen: Geological Magazine, v. 108, no. 1, p. 27-42.

Henry, C.D., and McDowell, F.W., 1986, Geochronology of magmatism in the Tertiary volcanic field, Trans-Pecos Texas, in Price, J.G., and others, eds., Igneous geology of Trans-Pecos Texas: Field Trip guide and research articles: University of Texas, Austin, Bureau of Economic Geology Guidebook 23, p. 99-122.

Henry, C.D., and Price, J.G., 1984, Variations in caldera development in the Tertiary volcanic field of Trans-Pecos Texas: Journal of Geophysical Research, v. 89, no. B10, p. 8765-8786.

Huffington, R.M., 1943, Geology of the northern Quitmans, Trans-Pecos Texas: Geological Society of America Bulletin, v. 54, no. 7, p. 987-1048.

Jones, B.R., 1968, Geology of southern Quitman Mountains and vicinity, Hudspeth County, Texas: Texas A&M, College Station, Ph.D. dissertation, 162 p.

Jones, B.R., and Reaser, D.F., 1970, Geology of southern Quitman Mountains, Hudspeth County, Texas: Texas University Bureau of Economic Geology quadrangle map no. 39, text.

King, P.B., 1965, Geology of the Sierra Diablo region, Texas: U.S. Geological Survey Professional Paper 480, 185 p.

King, P.B., and Flawn, P.T., 1953, Geology and mineral deposits of Precambrian rocks of the Van Horn area, Texas: Texas University Bureau of Economic Geology Publication 5301, 218 p.

Kluth, C.E., and Coney, P.J., 1981, Plate tectonics of the Ancestral Rocky Mountains: Geology, v. 9, no. 1, p. 10-15.

Lipman, P.W., Prostka, H.J., and Christiansen, R.L, 1972, Cenozoic volcanism and plate tectonic evolution of the western United States: I. Early and middle Cenozoic: Royal Society of London Philosophical Transactions, ser. A, v. 271-248.

McKinney, R.G., 1986, Personal communication, Gila Exploration, Sante Fe, New Mexico.

Morley, C.K., 1986, A classification of thrust fronts: American Association of Petroleum Geologists Bulletin, v. 70, no. 1, p. 12-25.

Muehlberger, W.R., Denison, R.E., and Lidiak, E.G., 1967, Basement in the continental interior of the United States: American Association of Petroleum Geologists Bulletin, v. 51, no. 12, p. 2351-2380.

Price, J.G., and Henry, C.D., 1984, Stress orientations during Oligocene volcanism in Trans-Pecos Texas: Timing the transition from Laramide compression to Basin and Range tension: Geology, v. 12, no. 4, p. 238-241.

Reaser, D.F., 1974, Geology of Cieneguilla area, Chihuahua and Texas: University of Texas, Austin, Ph.D. dissertation, 340 p.

Reaser, D.F., 1982, Geometry and deformational environment of the Cieneguilla-Quitman range in northeastern Chihuahua, Mexico, and western Trans-Pecos Texas, U.S.A., in Powers, R.B., ed., Geologic studies of the Cordilleran thrust belt, v. 1: Rocky Mountain Association of Geologists, Denver, Colorado, p. 425-450.

Reaser, D.F., and Underwood, J.R., Jr., 1975, Tectonic style of the Eagle-Southern Quitman Mountains region, western Trans-Pecos Texas: Society of Economic Paleontologists and Mineralogists, Permian Basin Section, Publication 75-15, p. 95-102.

Reynolds, D., 1985, Deformation along the late Precambrian Streeruwitz thrust near Allamore, Hudspeth County, Texas, in Dickerson, P.W., and Muehlberger, W.R., eds., Structure and tectonics of Trans-Pecos Texas: West Texas Geological Society Publication 85-71, p. 107-115.

Robertson, E.C., 1960, Creep of Solenhofen Limestone under moderate hydrostatic pressure, in Griggs, D., and Handin, J., eds, Rock deformation: Geological Society of America Memoir 79, p. 227-244.

Silver, L.T., and Anderson, T.H., 1974, Possible left-lateral early to middle Mesozoic disruption of the southwestern North American craton margin (abs): Geological Society of America Abstracts with Programs, v. 6, no. 7, p. 955-956.

Smith, J.F., Jr., 1940, Stratigraphy and structure of the Devil Ridge area, Texas: Geological Society of America Bulletin, v. 51, no. 4, p. 597-638.

Stewart, J.H., 1976, Late Precambrian evolution of North America: Plate tectonic implication: Geology, v. 4, no. 1, p. 11-15.

Twiss, P.C., 1959a, Geology of Van Horn Mountains, Texas: Texas University Bureau of Economic Geology quadrangle map no. 23, text.

Twiss, P.C., 1959b, Geology of Van Horn Mountains, Texas: University of Texas, Austin, Ph.D. dissertation, 234 p.

Underwood, J.R., Jr., 1962, Geology of Eagle Mountains and vicinity, Trans-Pecos Texas: University of Texas, Austin, Ph.D. dissertation, 560 p.

Underwood, J.R., Jr., 1963, Geology of Eagle Mountains and vicinity, Trans-Pecos Texas: Texas University Bureau of Economic Geology quadrangle map no. 26, text.

Zoback, M.L, Anderson, R.E., and Thompson, G.A., 1981, Cainozoic evolution of the state of stress and style of tectonism of the Basin and Range province of the western United States: Royal Society of London Philosophical Transactions, ser. A, v. 300, p. 407-434.

APPENDICES

APPENDIX 1

Detailed Description of Folds in the Black Butte area

Speck Ridge Fold Area

Several folds with axial traces greater than one km, are located to the northeast and southwest of Speck Ridge (Plate 1). An asymmetrical syncline, trending N. 40° W. and plunging to the southeast is located approximately 1060 m northeast of the northern part of Speck Ridge. The Espy Limestone is exposed in two separate outcrops in the northwestern (H-10) and southeastern (I-11) parts of the fold. The similar trend and alignment of the axial trace and the similar plunge (10°-15°) of the fold axis in these two separate outcrops correlates them as parts of the same fold. This syncline is asymmetrical to the southwest.

An anticline-syncline pair trending approximately N. 35° W. and plunging to the southeast is located just to the northeast of the northern part of Speck Ridge; the southwestern limb of the syncline forms the northeastern half of Speck Ridge. Beds of the Finlay Limestone are exposed along the length of the syncline, which is asymmetrical to the northeast, and along most of the length of the anticline, also asymmetrical to the northeast. In the northwestern part of the anticline (H-8), the Cox Sandstone, in the core of the fold, is exposed and the

anticline is overturned, the northeast limb dipping 84° to the southwest.

A southeast-plunging syncline, trending N. 45° W., plunges southeast beneath Black Butte. The Espy Limestone is exposed in two outcrops in the northwestern and southeastern parts of the syncline, to the northwest and southeast of Black Butte, respectively. Finlay Limestone, dipping steeply to the northeast, is exposed along the southwestern limb of the syncline and forms the northeastern half of the southern part of Speck Ridge. This syncline is asymmetrical to the northeast and is probably a southeast extension of the syncline located just to the northeast of the northern part of Speck Ridge. Steeply dipping, overturned strata of the Finlay Limestone and Cox Sandstone form the southwestern half of Speck Ridge. These overturned beds form the northeast limb of a large, overturned anticline trending northwest, the axial trace of which is not exposed but which must lie southwest of Speck Ridge. The limestone that crops out to the southwest of Speck Ridge (J,K-3,4 and K,L-6,7) may be part of the southwest limb of this anticline or part of a separate fold. The overturned limb of this anticline is in contact with the southwestern limb of the syncline to the northeast along a fault that traverses the length of Speck Ridge.

An east-to-east-northeast-trending strike-slip fault transects the southern part of Speck Ridge north of Judge

triangulation station (K-10). North of this fault and southwest of the normal fault that traverses the length of the ridge, beds of Cox and Finlay are overturned. South of this fault the same beds are not overturned, but dip to the east-southeast approximately 30°.

Northwestern Fold Area

In the northwest part of the study area, several northwest-trending folds occur in scattered exposures of the Bluff Formation, Yucca Formation, and Finlay Limestone.

A tight anticline-syncline fold pair in the southwestern part of this area (I-2) trends N. 20°-55° W. and occurs in an outcrop of limestone of the Bluff Formation. The anticline is asymmetrical to the northeast throughout its extent and plunges 5° southeast. The adjacent syncline is asymmetrical to the northeast in the southern part of the fold and overturned to the southwest in the northern part of the fold.

East-northeast of this outcrop (H-5), a north-northwest-trending syncline is located in a small exposure of Finlay Limestone (Section A-A'; Plate 2). This syncline trends N. 10°-25° W., plunges 15° southeast, and is asymmetrical to the northeast. Approximately 140 m east of this outcrop is a second small exposure of Finlay Limestone where the beds dip steeply to the east-northeast. These beds represent the northeastern limb of a north-northwest-

trending anticline, the axis of which is not exposed.

In the northwest corner of the study area, a series of northwest-trending, southeast-plunging folds are located in an outcrop composed of beds of the Yucca and Bluff formations. The westernmost fold of this series (F,G-2) is a syncline trending N. 15°-30° W. and plunging gently to the southeast. A strike-slip fault trending N. 65° E. offsets this syncline approximately halfway along the axial trace of the fold. North of this fault, the syncline is asymmetrical to the northeast. Immediately south of the fault, the syncline is overturned to the northeast. At the southwest tip of the outcrop, the beds of Bluff on the southwest limb of the syncline are dipping 63° to the northeast, and the northeast limb is not exposed. Therefore, the fold at this location is not overturned, unless beds of the unexposed northeast limb are overturned. The overturned syncline in the exposure of limestone of the Bluff Formation to the south of this outcrop may be an extension of this syncline, even though the syncline to the south is overturned in the opposite direction.

Northeast of the syncline is a northwest-trending anticline plunging to the southeast and asymmetrical to the northeast. Beds of the Yucca Formation are exposed along much of the axial trace. This fold is also offset by the northeast-trending strike-slip fault.

Farther northeast, two northwest-trending synclines

have been juxtaposed along a northwest-trending, high-angle fault. The syncline to the southwest is asymmetrical to the southwest, whereas the syncline to the northeast is asymmetrical to the northeast. An anticline trending N. 10° W. is located at the southeastern tip of this outcrop (G-3) and is asymmetrical to the northeast. In the northeastern corner of this outcrop (E-3), an anticline trending N. 32° W. is located with beds of the Yucca Formation exposed along much of its axial trace.

Northeast of this series of folds, limestone beds of the Bluff Formation have been folded into an anticline, asymmetrical to the southwest (E-4,5). This anticline trends N. 30° W. at its northern end and nearly due south at its southern end where it plunges 22°.

Approximately 230 m east of this exposure is another outcrop of the Bluff Formation, where beds have been folded into a syncline asymmetrical to the southwest, the axis of which trends N. 28° W. and plunges 5° southeast (E-5).

Pagoda Hill Fold Area

The Pagoda Hill fold area consists of folds located within 1500 m of the summit of Pagoda Hill (Plate 1). Units involved in the folding in this area include the Yucca, Bluff, and Chispa Summit formations.

In the immediate vicinity of Pagoda Hill, folds asymmetrical to the southwest and plunging to the northwest

are located within beds of the Yucca Formation. An anticline, trending N. 43° W. and plunging 3° to the northwest, is located east of Pagoda Hill (E-9). An anticline-syncline fold pair is located west of Pagoda Hill (E-8,9). The anticline trends N. 63° W. and plunges 10° northwest, and the syncline trends N. 55° W. and plunges 8° to the northwest.

Approximately 1200 m southwest of Pagoda Hill, an anticline-syncline fold pair is located within beds of the Bluff Formation (F,G-8). Both folds trend N. 13° W. and plunge approximately 5° to the southeast. The folds are located in the overthrust block of a northeast-trending thrust fault.

A northwest-trending anticline and syncline are located approximately 1100 m south-southeast of Pagoda Hill (G-9), within beds of the Bluff Formation. These folds are on opposite sides of a northwest-trending, southwest-dipping thrust fault. The anticline, on the overthrust block, is asymmetrical to the southwest and plunges 5° to the southeast. The syncline, on the underthrust block, is asymmetrical to the northeast and plunges 20° to the southeast.

A syncline, trending N. 18° W. and plunging 24° to the southeast, is located approximately 850 m southeast of Pagoda Hill (F-10), within beds of the Bluff Formation. This syncline is subparallel to several thrust faults

located just to the west.

Minor, unmapped folds approximately 1600 m northeast of Pagoda Hill (D-11,12) involve shale and limestone of the Chispa Summit Formation. These folds have amplitudes and wavelengths only of a few meters and trend, on the average, N. 80° W. and plunge 20° to the southeast. These folds located some 475 m north of the Devil Ridge thrust fault, are in the footwall block of that fault.

Horse Canyon Fold Area

The Horse Canyon fold area comprises folds in the western part of the study area and within 3 km of Horse Canyon and not included in the fold areas previously described. Rock units involved in the folds in this area include the Finlay Limestone, Cox Sandstone, and Bluff Formation.

A large anticline of Finlay Limestone is located in the extreme western part of this area, approximately 1740 m due north of Black Butte (G-11). This anticline trends N. 35°-58° W., plunges 3° to the southeast, and is asymmetrical to the southwest. Northeast of this anticline is a synlcine trending N. 55° W. and asymmetrical to the southwest. Both of these folds terminate abruptly to the northwest against an east-west-trending, high-angle fault. A northwest-trending fault on the southwest limb of the anticline separates the more steeply-dipping beds to the southwest

from the more gently-dipping beds to the northeast (Section C-C'; Plate 2).

To the northeast of these folds is a pair of folds in the Bluff Formation (F,G-12,13). An anticline to the southwest trending N. 42° W. is asymmetrical to the southwest and a syncline to the northeast, trending N. 50° W. is asymmetrical to the northeast. The anticline plunges 21° to the southeast and the syncline plunges 7° to the southeast.

A series of southeast-plunging folds just west of Horse Canyon (F,G-14,15) involve beds of the Bluff Formation and Cox Sandstone. The westernmost fold of this series is an anticline trending N. 22° W. and asymmetrical to the northeast (F,G-14). Beds of the Bluff Formation and Cox Sandstone crop out on the southwest limb. A northwest-trending thrust fault, dipping to the southwest, separates this anticline from the syncline to the northeast. Beds of the Bluff Formation of the northeast limb of the anticline, dipping approximately 60° to the east-southeast, are thrust against beds of Cox Sandstone of the southwest limb of the syncline, dipping approximately 30° to the east-southeast. The syncline is asymmetrical to the southwest and trends N. 8°-33° W. A northwest-trending, high-angle fault displaces beds on the northeast limb, placing the southwest-dipping beds of Bluff southwest of the fault into contact with southwest-dipping beds of Cox Sandstone northeast of the

fault. East-northeast of this syncline is an anticline asymmetrical to the southwest and trending N. 35° W. A syncline trending N. 60° W. is located at the east end of the ridge and is asymmetrical to the southwest. The two easternmost folds are located in the Bluff exposed in the ridge just west of Horse Canyon (F-15).

Two subparallel, northwest-trending, southwest-dipping thrust faults (F,G-15) separate these folds from the syncline to the west. These faults are parallel to sub-parallel to the thrust fault to the west and most of the folds in this area. The folds and faults are truncated on the northwest and southeast by east-northeast-trending, high-angle faults (Plate 1).

STRUCTURAL GEOLOGY OF BLACK BUTTE AREA, NORTHWEST EAGLE MOUNTAINS, HUDSPETH COUNTY, TEXAS

by

Donald Dean Edds

B. S., Fort Hays State University, 1984

AN ABSTRACT OF A MASTER'S THESIS

submitted in partial fulfillment of the

requirements for the degree

MASTER OF SCIENCE

Department of Geology

Kansas State University
Manhattan, Kansas

1987

ABSTRACT

The Black Butte area, mapped geologically at a scale of 1:24,000, is located on the northwest flank of the Eagle Mountains in southeastern Hudspeth County Texas and is an area of complexly faulted and folded Cretaceous sedimentary rock bounded on the southeast by the Tertiary volcanic rocks of the Eagle Mountains. Tertiary intrusive rocks and Quaternary sediments also occur in the area. The estimated 2,500 m of Cretaceous rock exposed in the study area consists of alternating siliciclastic and calciclastic units that were deposited along the eastern margin of the Chihuahua trough.

The dominant northwest structural trend in the area, represented mostly by fold and thrust-fault orientations, was produced during the Laramide Orogeny as northeast-southwest-oriented compression deformed the sediments of the trough. Folds are generally open and concentric, asymmetrical to overturned and are indicative of a near-surface deformational environment characterized by low-to-moderate pressure and low temperature. Thrust faults within the thrust sheet are arranged in an imbricate-fan pattern and show displacments ranging from a few tens to a few hundred meters. The Devil Ridge fault at the leading edge of the thrust sheet has a displacement estimated to be almost 6 km. Minor movement along northeast-trending

strike-slip faults accompanied the folding and thrust faulting.

Numerous, northeast-trending normal faults were superimposed on the Laramide structures as the region was uplifted and block faulted in the mid-Tertiary. These faults show displacements ranging from a few meters to several hundred meters and probably originated as shear fractures during Laramide compression. Normal movement has also occurred along a few northwest-trending faults that are believed to have originated as thrust faults during the Laramide Orogeny.

A significant difference in the type and degree of Laramide deformation between the Black Butte area and the Cieneguilla area 20 km to the south is attributed to the presence of a much thicker Permo-Jurassic(?) evaporite sequence, serving as a zone of dislocation for décollement-style tectonics and as an active element in the development of large-scale, complex folds in the Cieneguilla area.

Plate 1

GEOLOGIC MAP OF BLACK BUTTE AREA, NORTHWEST EAGLE MOUNTAINS, HUDSPETH COUNTY, TEXAS

BY DONALD D. EDDS

1987

105° 08' 05"
31° 00' 29"

30° 56' 39"
105° 13' 40"

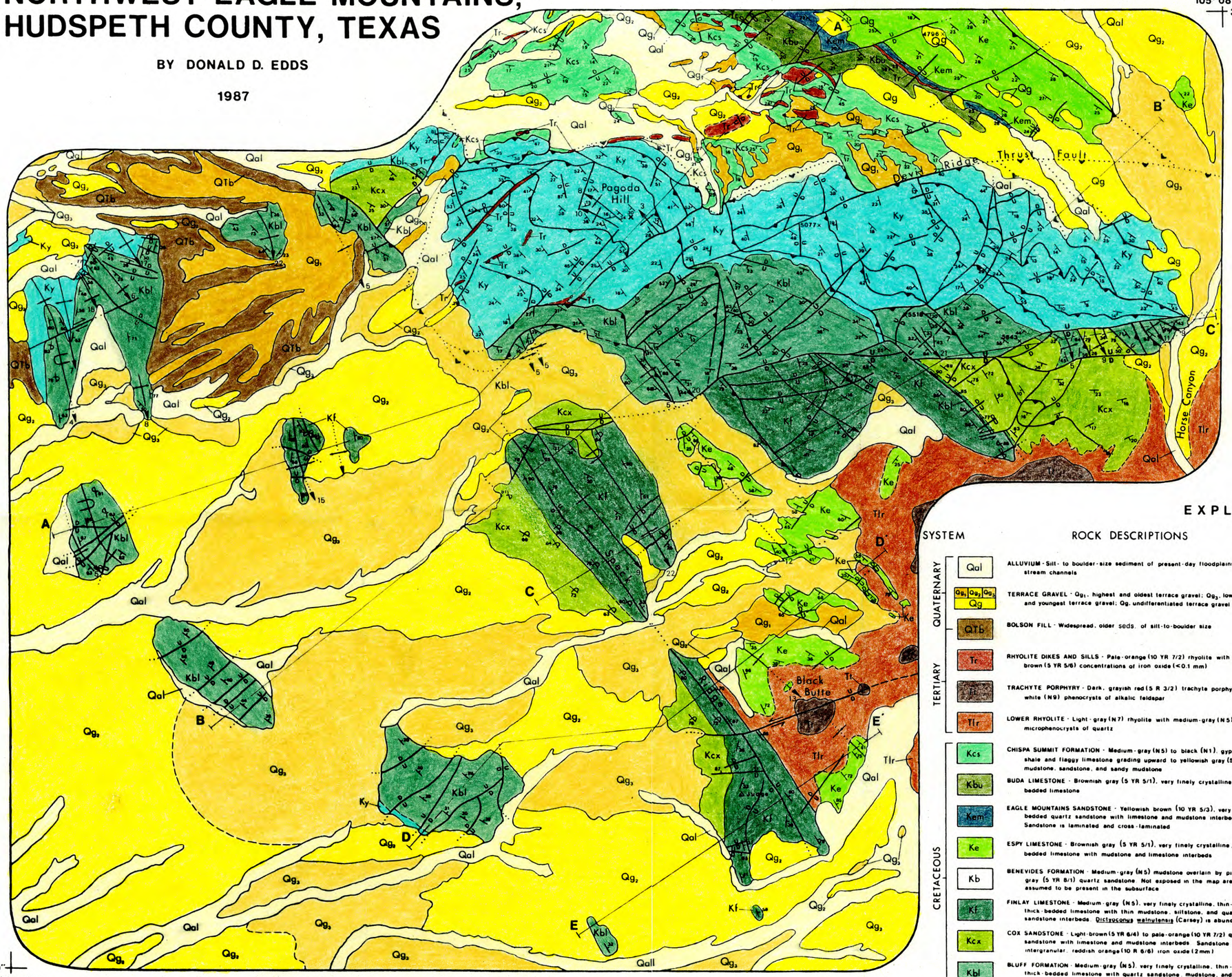

EXPLANATION

SYSTEM		ROCK DESCRIPTIONS
QUATERNARY	Qal	ALLUVIUM - Silt- to boulder-size sediment of present-day floodplains and stream channels
	Qg_3 Qg_2 Qg_1 Qg	TERRACE GRAVEL - Qg_1, highest and oldest terrace gravel; Qg_3, lowest and youngest terrace gravel; Qg, undifferentiated terrace gravel
TERTIARY	QTb	BOLSON FILL - Widespread, older seds. of silt-to-boulder size
	Tr	RHYOLITE DIKES AND SILLS - Pale-orange (10 YR 7/2) rhyolite with light-brown (5 YR 5/6) concentrations of iron oxide (<0.1 mm)
	Tt	TRACHYTE PORPHYRY - Dark, grayish red (5 R 3/2) trachyte porphyry with white (N9) phenocrysts of alkalic feldspar
	Tlr	LOWER RHYOLITE - Light-gray (N7) rhyolite with medium-gray (N5) microphenocrysts of quartz
CRETACEOUS	Kcs	CHISPA SUMMIT FORMATION - Medium-gray (N5) to black (N1), gypsiferous shale and flaggy limestone grading upward to yellowish gray (5 Y 8/1) mudstone, sandstone, and sandy mudstone
	Kbu	BUDA LIMESTONE - Brownish gray (5 YR 5/1), very finely crystalline, thin-bedded limestone
	Kem	EAGLE MOUNTAINS SANDSTONE - Yellowish brown (10 YR 5/3), very thin-bedded quartz sandstone with limestone and mudstone interbeds. Sandstone is laminated and cross-laminated
	Ke	ESPY LIMESTONE - Brownish gray (5 YR 5/1), very finely crystalline, thin-bedded limestone with mudstone and limestone interbeds
	Kb	BENEVIDES FORMATION - Medium-gray (N5) mudstone overlain by pinkish gray (5 YR 8/1) quartz sandstone. Not exposed in the map area but assumed to be present in the subsurface
	Kf	FINLAY LIMESTONE - Medium-gray (N5), very finely crystalline, thin- to thick-bedded limestone with thin mudstone, siltstone, and quartz-sandstone interbeds. Dictyoconus walnutensis (Carsey) is abundant
	Kcx	COX SANDSTONE - Light-brown (5 YR 6/4) to pale-orange (10 YR 7/2) quartz sandstone with limestone and mudstone interbeds. Sandstone contains intergranular, reddish orange (10 R 6/6) iron oxide (2 mm)
	Kbl	BLUFF FORMATION - Medium-gray (N5), very finely crystalline, thin- to thick-bedded limestone with quartz sandstone, mudstone, and oolitic limestone interbeds. Orbitolina sp. is abundant
	Ky	YUCCA FORMATION - Quartz sandstone, conglomeratic sandstone, and conglomerate grading upward to sandstone, siltstone, mudstone, and limestone. Distinctive reddish brown (10 R 4/4) color

SYMBOLS

- CONTACT - Dashed where inferred
- THRUST FAULT - Sawteeth on upper plate; dashed where inferred, dotted where concealed
- STRIKE-SLIP FAULT - Showing relative horizontal movement, dashed where inferred, dotted where concealed
- HIGH-ANGLE FAULT - Showing dip; U, upthrown side; D, downthrown side; dashed where inferred, dotted where concealed
- ANTICLINE - Showing direction of plunge; dotted where concealed
- OVERTURNED ANTICLINE - Showing direction of dip of limbs; dotted where concealed
- SYNCLINE - Showing direction of plunge; dotted where concealed
- OVERTURNED SYNCLINE - Showing direction of dip of limbs; dotted where concealed

STRIKE AND DIP OF BEDS

25 Inclined 80 Vertical 78 Overturned

- TRIANGULATION STATION
- A — A' LINE OF CROSS-SECTION

Base map from U.S. Geological Survey 7.5-minute topographic quadrangles

Grayton Lake (1983), C.I. - 10 feet
Eagle Mountains NW (1972), C.I. - 40 feet

SCALE

0 0.25 0.5 1 MILES

0 0.25 0.5 1 KILOMETERS

TN MN
11½°

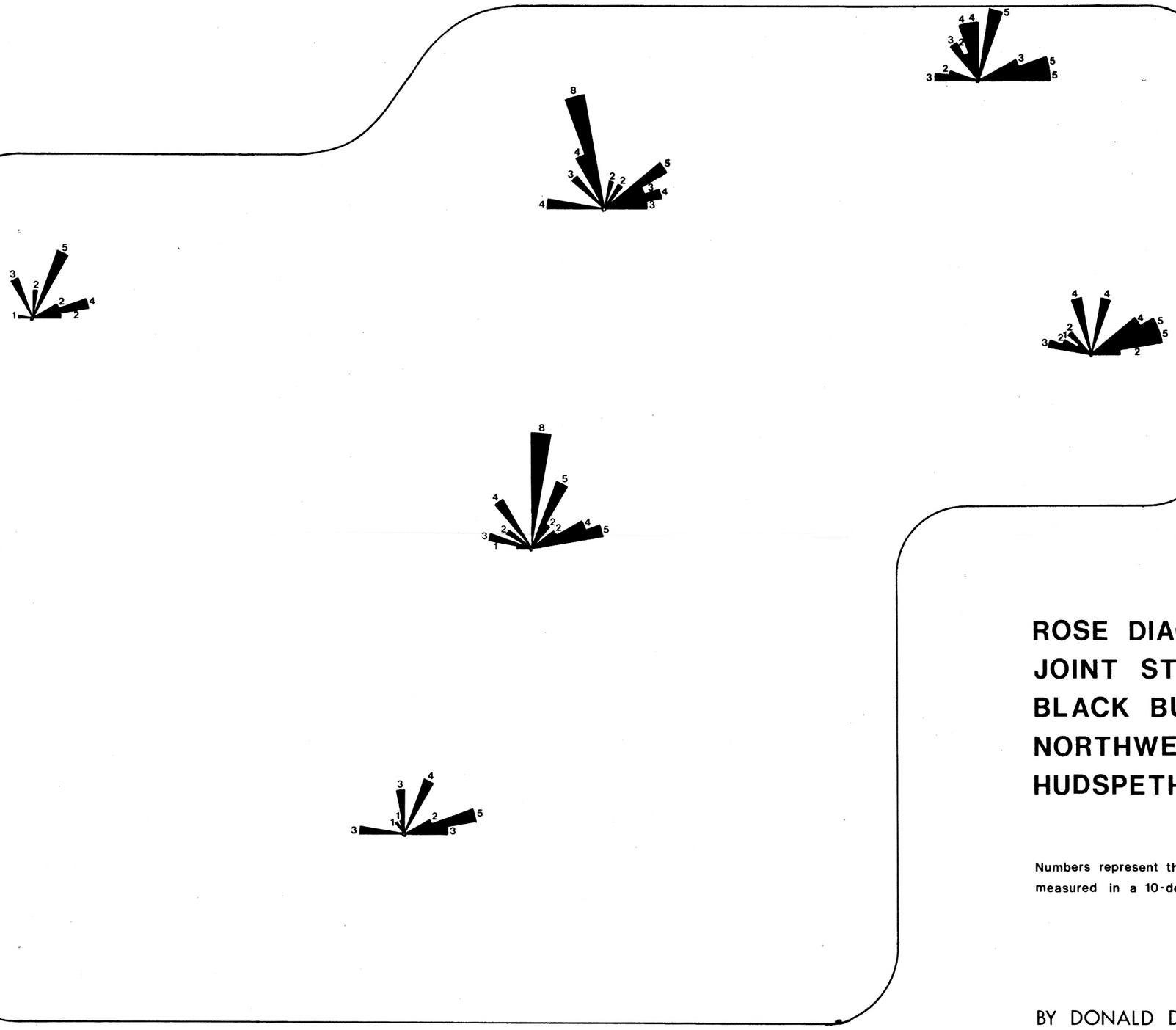

SCALE

0 0.25 0.5 1 MILES

0 0.25 0.5 1 KILOMETERS

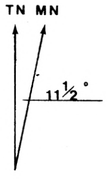

ROSE DIAGRAMS OF JOINT STRIKES IN BLACK BUTTE AREA, NORTHWEST EAGLE MOUNTAINS, HUDSPETH COUNTY, TEXAS

Numbers represent the actual number of joint strikes measured in a 10-degree interval

BY DONALD D. EDDS

1987

GEOLOGIC CROSS SECTIONS IN BLACK BUTTE AREA, NORTHWEST EAGLE MOUNTAINS, HUDSPETH COUNTY, TEXAS

BY DONALD D. EDDS

1987

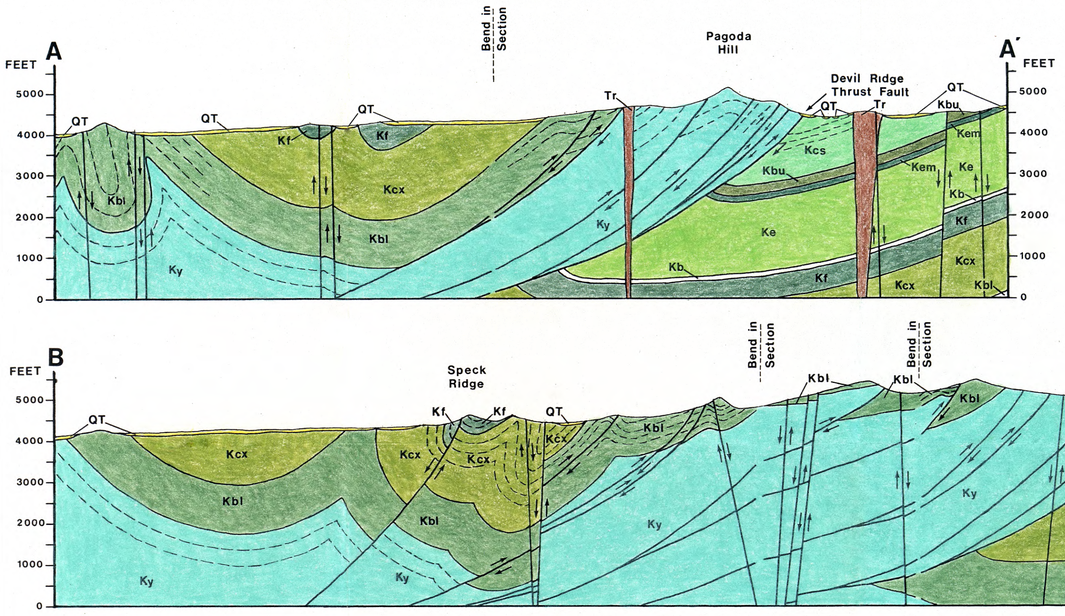

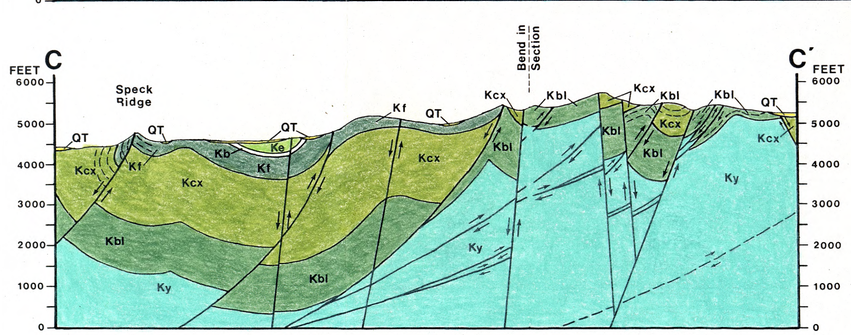

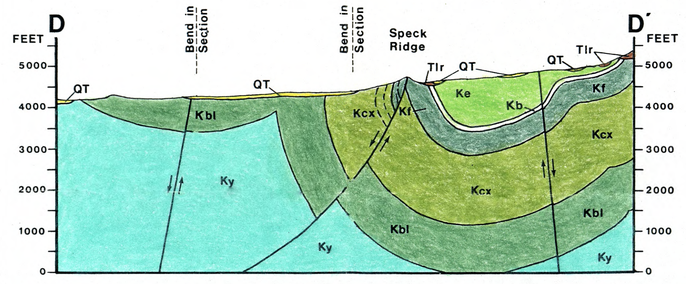

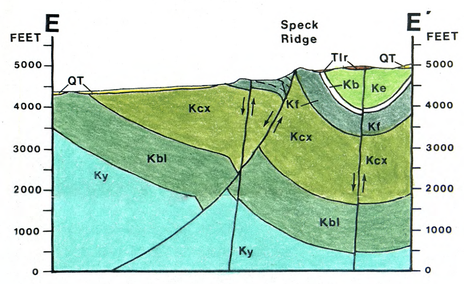

EXPLANATION

ROCK UNITS

- QT — Undifferentiated Quaternary and Tertiary sediments
- Tr — Rhyolite dikes and sills
- Tlr — Lower Rhyolite
- Kcs — Chispa Summit Formation
- Kbu — Buda Limestone
- Kem — Eagle Mountains Sandstone
- Ke — Espy Limestone
- Kb — Benevides Formation
- Kf — Finlay Limestone
- Kcx — Cox Sandstone
- Kbl — Bluff Formation
- Ky — Yucca Formation

SYMBOLS

- FAULT - Showing relative vertical movement; dashed where inferred
- FORM LINES
- CONTACT

NO VERTICAL EXAGGERATION

SCALE

0 0.5 1 2 MILES

0 0.5 1 2 KILOMETERS